Jak2^{V617F} Reversible Activation Shows Its Essential Requirement in Myeloproliferative Neoplasms

Andrew J. Dunbar,†[1,2,3] Robert L. Bowman,†[1] Young C. Park,[1] Kavi O'Connor,[1] Franco Izzo,[4,5] Robert M. Myers,[4,5] Abdul Karzai,[1] Zach Zaroogian,[1] Won Jun Kim,[1] Inés Fernández-Maestre,[1,6] Michael R. Waarts,[1,6] Abbas Nazir,[1] Wenbin Xiao,[1,7] Tamara Codilupi,[8] Max Brodsky,[1,9] Mirko Farina,[1,10] Louise Cai,[1] Sheng F. Cai,[1,2] Benjamin Wang,[1] Wenbin An,[11] Julie L. Yang,[12] Shoron Mowla,[1] Shira E. Eisman,[1] Amritha Varshini Hanasoge Somasundara,[1] Jacob L. Glass,[1,2,12] Tanmay Mishra,[1] Remie Houston,[1] Emily Guzzardi,[1] Anthony R. Martinez Benitez,[1] Aaron D. Viny,[13] Richard P. Koche,[12] Sara C. Meyer,[8,14] Dan A. Landau,[4,5] and Ross L. Levine*[1,2,3,12]

†These authors contributed equally to this work

[1]Human Oncology & Pathogenesis Program, Memorial Sloan Kettering Cancer Center, New York, NY 10065, USA.
[2]Leukemia Service, Department of Medicine and Center for Hematologic Malignancies, Memorial Sloan Kettering Cancer Center, New York, 10065 NY, USA.
[3]Myeloproliferative Neoplasm-Research Consortium.
[4]Weill Cornell Medical College of Cornell University, New York, NY 10065, USA.
[5]New York Genome Center, New York, NY 10013, USA
[6]Louis V. Gerstner Jr Graduate School of Biomedical Sciences, Memorial Sloan Kettering Cancer Center, New York, NY, USA.
[7]Department of Pathology, Memorial Sloan Kettering Cancer Center, New York, NY, USA.
[8]Department of Biomedicine, University of Basel, Basel, Switzerland
[9]Department of Medicine, Johns Hopkins University School of Medicine, Baltimore, Maryland, USA.
[10]Unit of Blood Diseases and Bone Marrow Transplantation, Cell Therapies and Hematology Research Program, University of Brescia, ASST Spedali Civili di Brescia, Italy
[11]State Key Laboratory of Experimental Hematology, National Clinical Research Center for Blood Diseases, Institute of Hematology & Blood Diseases Hospital, Chinese Academy of Medical Sciences & Peking Union Medical College, Tianjin, China.
[12]Center for Epigenetics Research, Memorial Sloan Kettering Cancer Center, New York, NY, USA.
[13]Columbia Stem Cell Initiative and Department of Medicine, Division of Hematology & Oncology, Columbia University Medical Center, New York, NY, USA
[14]Department of Hematology and Central Hematology Laboratory, Inselspital, Bern University Hospital, University of Bern, Bern, Switzerland

***Corresponding Author:** Dr. Ross L. Levine
Mailing: 1275 York Ave, Box 20, New York, NY 10065
E-mail: leviner@mskcc.org
Phone: 646-888-2747
Fax: 646-422-0890

Running Title: Oncogenic dependency of JAK2^{V617F} in MPNs

Keywords: Myeloproliferative Neoplasms, Mouse Models, Oncogenic Signaling, JAK2, Ruxolitinib

Word count: 4,158

Figures and Tables: 4

Conflict of interest statement: R.L.L. is on the supervisory board of Qiagen and is a scientific advisor to Imago, Mission Bio, Bakx, Zentalis, Ajax, Auron, Prelude, C4 Therapeutics and Isoplexis. He has received research support from Abbvie, Constellation, Ajax, Zentalis and Prelude. He has received research support from and consulted for Celgene and Roche and has consulted for Syndax, Incyte, Janssen, Astellas, Morphosys and Novartis. He has received honoraria from Astra Zeneca and Novartis for invited lectures and from Gilead and Novartis for grant reviews. S.C.M. has consulted for and received honoraria from Celgene/BMS, Novartis, GSK and OrPha Swiss and receives research support from Ajax. D.A.L. is on the Scientific Advisory Board of Mission Bio, Alethiomics, Pangea, Quotient Therapeutics and C2i Genomics and has received prior research funding from BMS, 10X Genomics, Mission Bio, Ultima Genomics, Oxford Nanopore and Illumina unrelated to the current manuscript. S.F.C. was a consultant for and previously held equity interest in Imago Biosciences, none of which are directly related to the content of this paper. A.D. has served on an advisory board for Incyte. R.L.B. has received honoraria from Mission Bio and is a member of the Speakers Bureau for Mission Bio. No other authors report competing interests.

ABSTRACT (149 words)

Gain-of-function mutations activating JAK/STAT signaling are seen in the majority of patients with myeloproliferative neoplasms (MPNs), most commonly JAK2^{V617F}. While clinically-approved JAK inhibitors improve symptoms and outcomes in MPNs, remissions are rare, and mutant allele burden does not substantively change with chronic therapy. We hypothesized this is due to limitations of current JAK inhibitors to potently and specifically abrogate mutant JAK2 signaling. We therefore developed a conditionally inducible mouse model allowing for sequential activation, and then inactivation, of *Jak2*^{V617F} from its endogenous locus using a combined, Dre-*rox*/Cre-*lox* dual recombinase system. *Jak2*^{V617F} deletion abrogates MPN features, induces depletion of mutant-specific hematopoietic stem/progenitor cells, and extends overall survival to an extent not observed with pharmacologic JAK inhibition, including when co-occurring with somatic *Tet2* loss. Our data suggest JAK2^{V617F} represents the best therapeutic target in MPNs and demonstrate the therapeutic relevance of a dual-recombinase system to assess mutant-specific oncogenic dependencies *in vivo*.

STATEMENT OF SIGNIFICANCE (50 words)

Current JAK inhibitors to treat myeloproliferative neoplasms are ineffective at eradicating mutant cells. We developed an endogenously-expressed *Jak2*^{V617F} dual-recombinase knock-in/knock-out model to investigate *Jak2*^{V617F} oncogenic reversion *in vivo*. *Jak2*^{V617F} deletion abrogates MPN features and depletes disease-sustaining MPN stem cells suggesting improved *Jak2*^{V617F} targeting offers the potential for greater therapeutic efficacy.

INTRODUCTION

Somatic mutations which constitutively activate JAK2 signaling are seen in the majority of myeloproliferative neoplasm (MPN) patients,(1) most commonly the recurrent JAK2^{V617F} alteration, and murine models suggest a critical role for JAK/STAT pathway mutations in promoting the MPN phenotype *in vivo*.(2-6) In contrast to ABL1 kinase inhibition in BCR-ABL1-driven chronic myelogenous leukemia,(7) current JAK inhibitors fail to reduce mutant clonal fraction, do not induce pathologic regression of key disease features including myeloproliferation and bone marrow fibrosis, and most patients lose their response over time.(8,9) To date, second-site JAK2 mutations have not been observed as a mechanism of acquired resistance,(10) and different mechanisms have been postulated to mediate the inadequate efficacy of JAK inhibition, including incomplete dependency on JAK2 signaling and the presence of co-occurring mutant disease alleles.(11) We hypothesized that the limited potency of JAK inhibition relates to insufficient mutant kinase inhibition at achievable therapeutic doses,(4,12) and we and others have elucidated mechanisms by which mutant JAK2 can signal in the presence of type I JAK inhibitors.(12-14) Previous model systems evaluating doxycycline-inducible *Jak2^{V617F}* expression highlight the importance of oncogenic JAK2^{V617F} signaling in sustaining the MPN phenotype;(6) however, these systems were limited by the inability to accurately recapitulate reversal of endogenous mutant expression or allow for assessment of oncogenic dependency on MPN hematopoietic stem cell (HSC) fitness alone or in context of co-mutations acquired during clonal evolution and myeloid transformation. Given this, we developed a system which would more definitively assess JAK2^{V617F} dependency in MPN.

RESULTS

A conditional knock-in, knock-out model of *Jak2^{V617F}* MPN

To assess the requirement for JAK2^{V617F} oncogenic signaling in MPN disease maintenance, we generated a Dre-*rox*,(15) Cre-*lox*(16) dual-recombinase *Jak2^{V617F}* knock-in/knock-out mouse model (*Jak2$^{Rox/Lox}$*/*Jak2^{RL}*) by gene targeting in mouse embryonic stem cells **(Figure 1A)**. The close proximity of the *lox* sites (82 base pairs) prevents Cre-mediated deletion prior to Dre-mediated recombination and *Jak2^{V617F}* induction. Once the mutant allele is activated, the *lox* sites separate allowing for subsequent Cre-mediated deletion of *Jak2^{V617F}*, including in models where cooperating alleles are induced by antecedent Cre-mediated activation/deletion. A similar strategy, which we have termed GOLDI-Lox for governing oncogenic loci by Dre inversion and

lox deletion, was also used to target *Flt3*^{ITD} (see Bowman, R. *et al.*, biorxiv.org [https://doi.org/10.1101/2022.05.18.492524], 2022). Given previous literature demonstrating that *Jak2* expression is essential for hematopoiesis,(17,18) all *Jak2*^{RL} mice used for experiments were heterozygous, with one maintained copy of the wild-type (WT) *Jak2* allele **(Supp Figure 1A)**. In the absence of Dre recombination, *Jak2*$^{RL/+}$ heterozygous mice displayed no observable phenotype, consistent with previous studies (not shown).(2,17-20) Sequencing of the *Jak2*^{RL} locus on sorted Cre reporter cells(21) after Cre recombinase exposure confirmed retainment of the non-recombined *Jak2*^{RL} locus **(Supp. Figure 1B)**. We transiently expressed Dre recombinase by mRNA electroporation *ex vivo* in primary lineage-negative bone marrow cells, efficiently inducing *Jak2*^{V617F} activation and separation of *lox* sites by inversion **(Supp. Figure 1C)**. Single-colony genotyping of these cells cultured in methylcellulose for 7 days revealed evidence of knock-in in 28-55% of assayed colonies (n = 33/replicate). Efficient *Jak2*^{V617F} mutant induction was also observed in lineage-negative bone marrow harvested from primary transplant donors 6 weeks following electroporation and transplant **(Supp. Figure 1D-E)**. By three weeks post-transplant, lethally irradiated mice transplanted with Dre-inducible *Jak2*^{RL} knock-in bone marrow developed a highly penetrant and fully transplantable MPN characterized by leukocytosis with myeloid preponderance, elevated hematocrit with erythroid progenitor expansion in bone marrow, hepatosplenomegaly, and megakaryocytic hyperplasia consistent with prior *Jak2*^{V617F} conditional knock-in mouse models of MPN **(Supp. Figure 1F-J)**.(3) Variable bone marrow fibrosis was observed across primary and secondary transplant recipient cohorts. While there was minimal evidence of fibrosis in primary recipient mice, in secondarily transplanted mice, by >16 weeks, we observed 0-2+ reticulin fibrosis in 14/23 (61%) mice across multiple independent non-competitive and competitive transplant studies (n = 5, **Supp. Figure 1K)**.

To assess the reversibility of the *Jak2*^{RL} construct, we cultured *Dre*-electroporated, lineage-negative, tamoxifen (TAM)-inducible *Ubc:CreER-Jak2*^{RL} cells isolated from donor mice with active MPN *ex vivo* with increasing doses of 4-hydroxy-tamoxifen (4-OHT) over bone marrow endothelial cells (BMECs) **(Supp. Figure 2A)**.(22) Treatment with 4-OHT resulted in deletion of the *Jak2*^{V617F} allele, which was confirmed by excision polymerase chain reaction (PCR) **(Supp. Figure 2B)**. Loss of *Jak2*^{V617F} significantly reduced cell numbers *ex vivo* (mean 4-OHT 0.18×10^6/mL vs. VEH 2.19×10^6/mL, $p \leq 0.0001$), including within immunophenotypically-defined hematopoietic stem/progenitor cell (HSPC) compartments, a phenotypic change not observed with vehicle (VEH)-treated *Jak2*^{RL}, Cre-inducible *Jak2*^{V617F} (*Jak2*^{Crelox}; $p \leq 0.228$),(2) or Cre-

inducible WT cells ($p \leq 0.114$) **(Supp. Figure 2C-G)**. Loss of *Jak2*^{V617F} also abrogated erythropoietin-independent erythroid differentiation(23) *in vitro* ($p \leq 0.01$) **(Supp. Figure 2H)**. The cell loss observed was associated with enhanced apoptosis, which was most apparent in Mac1^{+} mature myeloid cells (mean 4-OHT 35% vs. VEH 9.3%, $p \leq 0.005$) (**Supp. Figure 2I)**.

We next evaluated the impact of reversible *Jak2*^{V617F} expression *in vivo*. Twelve weeks post-transplant, secondary recipient mice transplanted with *Dre*-electroporated *Ubc:CreER-Jak2*^{RL} whole bone marrow and exhibiting MPN were administered TAM to delete *Jak2*^{V617F} **(Supp. Figure 3A)**. A sequential *rox*-stop-*rox*, *lox*-TdTomato-stop-*lox*-eGFP dual recombinase reporter system,(24) in which TdTomato is expressed following Dre and then TdTomato deletion with concomitant GFP+ induction is expressed following Cre, was used to validate *Jak2*^{V617F} deletion within Cd45.2 reporter-positive cell populations **(Supp. Figure 3B)**. Deletion of *Jak2*^{V617F} was also validated *in vivo* at the transcriptional level ($p \leq 0.0001$) **(Supp. Figure 3C)** and was associated with loss of constitutive JAK/STAT signaling **(Figure 1B)**. Consistent with our *in vitro* data, we observed normalization of white blood cell (WBC; mean TAM 6.18 K/uL vs. MPN 17.5 K/uL, $p \leq 0.0001$), hematocrit (Hct; mean 52.6% vs. 79.9%, $p \leq 0.01$), and platelet (mean 786 K/uL vs. 2146 K/uL, $p \leq 0.0004$) parameters within 4 weeks following TAM treatment that persisted until timed sacrifice at 24 weeks **(Figure 1C, Supp. Figure 3D)**. As early as 7 days post-TAM, we observed an increase in Annexin V+ cells (mean TAM 34.1% vs. MPN 8.4%, $p \leq 0.01$) in HSPC fractions consistent with an acute induction of apoptosis and concomitant reduction in the percentage of cycling HSPCs by flow (G2-M phase TAM 9.4% vs. MPN 14.9%, $p \leq 0.01$) **(Supp. Figure 3E-F)**. Two of 12 mice demonstrated reemergence/persistence of the MPN phenotype, both of which showed incomplete excision of the *Jak2*^{RL} allele highlighting the necessity of Jak2^{V617F} in disease maintenance **(Supp. Figure 3G)**. Wild-type *Jak2* mRNA levels were increased at 7 days following oncogenic reversion, an effect that was sustained at the protein level until timed sacrifice at 24 weeks, as evidenced by western blot of harvested splenocytes, suggesting a potential compensatory mechanism in response to oncogenic reversion **(Supp. Figure 3H-I)**. Genetic reversal of *Jak2*^{V617F} significantly prolonged overall survival (median not defined vs. 187 days, $p \leq 0.0012$) and led to loss of disease-defining MPN features in the majority of mice (9/12) **(Figure 1D)**. Spleen weights (mean 108.9 mg vs. 542.7 mg, $p \leq 0.0001$) were reduced, and we observed an overall trend in reduction of multiple inflammatory cytokines with *Jak2*^{V617F} reversal **(Figure 1E-F)**. Significant cytokine reductions, while similar to what has previously been seen in patient samples receiving ruxolitinib therapy,(25,26) including IL-6 (*FDR* ≤ 0.015) and MIP-1β (*FDR* ≤ 0.018), also showed

reductions in serum Eotaxin (*FDR* ≤ 0.024) at time of sacrifice and a trend towards reduction with IP-10 (*FDR* ≤ 0.067) **(Supp. Figure 3J)**. Histopathologic analysis of bone marrow and spleen revealed reductions in megakaryocytic hyperplasia, splenic infiltration, reduced overall cellularity, and absence of bone marrow and spleen fibrosis in 8 of 9 assayed *Jak2*^{V617F}-deleted mice that persisted until timed sacrifice at 24 weeks **(Figure 1G, Supp. Figure 3K)**. The phenotypes observed with *Ubc:CreER-Jak2*^{V617F} deletion *in vivo*, including the histologic effects, were not observed with TAM administration in the absence of *Jak2*^{V617F} reversal **(Supp. Figure 4A-G)**. We conclude that the MPN phenotype requires maintenance of oncogenic signaling through Jak2^{V617F}.

Jak2^{V617F} reversal impairs the fitness of MPN cells, including MPN HSCs

We next evaluated *Dre*-electroporated *Jak2*^{RL} bone marrow from Cd45.2 MPN donors in competition with Cd45.1 competitor cells to explore effects of *Jak2*^{V617F} deletion on peripheral blood and bone marrow mutant cell fitness **(Supp. Figure 5A)**. Both early (3 weeks post-transplant) or late (12 weeks) administration of TAM resulted in abrupt, durable reductions in Cd45.2 mutant cell fraction in the peripheral blood (mean 24.5% vs. 63.9%, $p \leq 0.001$), coinciding with normalization of hematologic parameters which persisted until time of sacrifice **(Figure 2A, Supp. Figure 5B)**. Consistent with the *in vitro* data, this effect was most pronounced in Mac1$^+$ myeloid cell fractions ($p \leq 0.0001$) **(Supp. Figure 5C)**. In bone marrow at timed sacrifice (24 weeks), the reductions in mutant cell fraction among the different HSPC compartments was more significant than that observed in peripheral blood, including within megakaryocytic-erythroid progenitor (MEP; Lineage$^-$cKit$^+$Sca1$^-$Cd34$^-$Fcg$^-$; $p \leq 0.0001$) and granulocytic-monocytic progenitor (GMP; Lineage$^-$cKit$^+$Sca1$^-$Cd34$^+$Fcg$^+$; $p \leq 0.0001$) populations and most importantly the LSK (Lineage$^-$cKit$^+$Sca1$^+$; $p \leq 0.0096$) stem cell compartment, including the SLAM-positive LSK population enriched for long-term hematopoietic stem cells (LT-HSCs; Lineage$^-$Sca1$^+$cKit$^+$Cd150$^+$Cd48$^-$; $p \leq 0.01$) **(Figure 2B, Supp. Figure 5D-F)**. Similar reductions in mutant cell fraction, as well as reductions in Ter119$^+$Cd71$^+$ erythroid precursors, were also observed in whole spleen ($p \leq 0.05$) in both early- and late-TAM cohorts consistent with an attenuation of extramedullary hematopoiesis **(Supp. Figure 5G-H)**. Recurrent MPN, as was seen in the non-competitive setting, was observed in 3 of 14 mice across both early- and late- treatment arms and corresponded with residual mutant *Jak2*^{V617F} expression and sustained mutant chimerism at sacrifice. We next queried mice without MPN, but persistent Cd45.2+ cells from this transplant. In 8/8 mice assayed, we observed neither *Jak2*^{V617F} knock-in nor *Jak2*^{V617F}

excision bands by PCR on sorted Cd45.2+ LSK cells (n = 3 early TAM, n = 5 late TAM) suggesting residual Cd45.2+ cells in these mice represent a non-Dre recombined *Jak2*^{RL} WT bystander cell population. Similar results were observed in a separate competitive transplant study; however, in 1/8 late TAM treated mice, we also observed a faint knock-in band despite no phenotypic evidence of MPN suggesting that in a minority of mice, residual mutant cells can remain and not necessarily give rise to disease **(Supp. Figure 5I)**. Transplant of unfractionated *Jak2*^{RL}-deleted bone marrow failed to form phenotypic disease in 4 of 5 secondary transplant recipient mice consistent with depletion of disease-propagating MPN HSCs **(Supp. Figure 5J-L)**.

We sought to characterize transcriptional changes following acute *Jak2*^{V617F} reversal. We performed RNA sequencing (RNA-Seq) analysis of purified HSPCs 3 and 7 days following *Jak2*^{V617F} deletion (n = 3-4) compared to MPN controls (n = 3-4). Transcriptional analysis of sorted, *Jak2*^{V617F}-deleted LSK and MEP populations revealed near-complete loss of expression of STAT5 target genes as early as 3 days post-deletion (LSK: NES -1.77, *FDR* $\leq$ 0.002; MEP: NES -1.53, *FDR* $\leq$ 0.0065) indicating immediate disengagement from disease-defining pathway signaling **(Supp. Figure 6A)**. By 7 days, we observed significant negative enrichment in IFNγ (NES -1.61, *FDR* $\leq$ 0.0005), TGFβ (NES -1.45, *FDR* $\leq$ 0.071), and TNFα via NFκB (NES -1.54, *FDR* $\leq$ 0.0017) Hallmark pro-inflammatory response pathways, as well as down-regulation of MAPK (NES -1.52, *FDR* $\leq$ 0.0052) and MTORC1 (NES -1.46, *FDR* $\leq$ 0.0071) targets in LSKs suggesting abrupt reduction in pro-inflammatory and proliferative signaling in the setting of *Jak2*^{V617F} deletion **(Figure 2C, Supp. Figure 6B, Supp. Table 1).** A flux towards increased expression of myeloid genes sets compared to erythroid gene sets was also observed at 7 days post-TAM initiation, characterized by increased *S100a8*, *S100a9*, *Mpo*, and *Hdc* expression in LSKs, increases in GMP (mean 14.5% vs. 7.8%, $p \leq 0.018$) vs. MEP (mean 13.8% vs. 32%, $p \leq 0.0025$) frequencies within the HSPC compartment, and enrichment in bone marrow Mac1^{+} myeloid cells (mean 41.7% vs. 27.8%, $p \leq 0.0084$) (**Figure 2D-E, Supp. Figure 6C)**. In line with reduced erythroid output, we also observed a marked decrease in heme metabolism in MEPs (NES -2.07, *FDR* $\leq 4.71 \times 10^{-5}$) with associated reductions in critical erythroid/megakaryocytic transcription factors and signaling mediators, including *Nfe3*,(27) *Plek2*,(28) and *EpoR*(29) which coincided with concomitant reductions in total erythroid progenitor cell numbers ($p \leq 0.021$) and significantly reduced burst forming unit-erythroid (BFU-E) colony output of *Jak2*^{V617F} deleted cells ($p \leq 0.001$) **(Figure 2F, Supp. Figure 6D-F)**. Assay for Transposase Accessible

Chromatin with high-throughput sequencing (ATAC-Seq) on *Jak2*^{V617F}-deleted cKit^{+} cells demonstrated an increase in open chromatin with Cebp motifs ($p \leq 1x10^{-10}$) and reduced accessibility at Gata motifs ($p \leq 1x10^{-620}$), including at critical erythroid loci (e.g. *EpoR*; log2FC 1.49, *FDR* ≤ 0.00135), further consistent with an erythroid to myeloid lineage switch **(Figure 2G, Supp. Figure 6G, Supp. Table 2)**. Lineage deconvolution(30) further suggested priming of cKit+ cells towards a monocyte-to-granulocyte maturation switch in the setting of oncogenic reversion, consistent with our flow cytometric data showing changes in lineage output before and after mutational reversion **(Supp. Figure 6H)**. While reduced accessibility at putative Gata target sites was observed, we did not observe differential expression of either *Gata1* ($p \leq 1.0$) or *Gata2* ($p \leq 0.82$) in *Jak2*^{V617F}-deleted LSKs or MEPs compared to controls. These data suggest the transcriptional networks regulating the MPN phenotype are not obligately achieved through transcription factor expression dysregulation but through differential transcription factor-mediated output.

Differential efficacy of *Jak2*^{V617F} deletion compared to JAK inhibitor therapy

Given the limited ability of current JAK inhibitors to achieve disease modification and/or clonal remissions in polycythemia vera and myelofibrosis (MF), we next compared the phenotypic and transcriptional effects of JAK inhibitor therapy with ruxolitinib to the effects of *Jak2*^{V617F} reversal. We first performed RNA-Seq on *Jak2*^{V617F}-mutant LSKs and MEPs following 7 days of ruxolitinib treatment ($n = 3$) and compared this to the effects of *Jak2*^{V617F} deletion ($n = 3$). JAK-STAT target gene expression and erythroid pathway gene expression were much less potently inhibited with ruxolitinib than with *Jak2*^{V617F} deletion. Specifically, *Jak2*^{V617F} deletion resulted in a significant reduction in JAK/STAT signaling (NES -1.51, $p \leq 0.003$) and expression of negative regulators including *Socs2*,(31) *Pim2*,(32) and *Cish.*(33) By contrast, ruxolitinib treatment was associated with a muted reduction in the same targets, with no significant changes in STAT5 target gene expression identified by GSEA (NES -0.913, $p = 0.84$) at this time point **(Figure 3A, Supp. Figure 7A, Supp. Table 3)**. Furthermore, the alterations in erythroid pathway gene expression in MEPs (NES 1.45, $p \leq 0.012$ vs. NES -1.82, $p \leq 0.0005$) and skewing of GMP and MEP frequencies observed with *Jak2*^{V617F} deletion were not observed with ruxolitinib (mean GMP: VEH 6.93% vs. ruxolitinib [RUX] 6.66% vs. TAM 20.1%, $p = 0.91$ vs. $p \leq 0.0001$, MEP: VEH 27.1% vs. RUX 35.3% vs. TAM 14.2%, $p = 0.25$ vs. $p = 0.014$) **(Figure 3B-C, Supp. Figure 7B-C)**. Expression of the gene sets associated with TGFβ ($p = 0.65$) and TNFα/NFκB (*p*

= 0.90) inflammatory signaling pathways also displayed minimal changes with ruxolitinib and were more potently downregulated with *Jak2*^{V617F} deletion. Consistent with this lack of change, genotype-aware single-cell ATAC-Seq (scATAC-Seq) on MF patient samples **(Supp. Table 4)** demonstrated unaltered NFκB accessibility in *JAK2*^{V617F}-mutant HSPCs following JAK inhibitor treatment **(Figure 3D, Supp. Figure 7D;** see Myers, R. and Izzo, F. *et al*., *Nature, in press,* 2024**)** supporting the notion of insufficient mitigation of inflammatory signaling by JAK inhibition on MPN-sustaining stem cells.

To evaluate the phenotypic effects of *Jak2*^{V617F} deletion in direct comparison to JAK kinase inhibition, we performed an *in vivo* trial lasting 6 weeks comparing ruxolitinib to *Jak2*^{V617F} deletion **(Supp. Figure 8A)**. We saw a greater improvement in hematologic parameters, spleen weights (mean VEH 457 mg vs. RUX 235 mg vs. TAM 125 mg, $p \leq 0.0027$), restoration of histopathologic morphology in both bone marrow and spleen, and reduced Cd45.2 mutant chimerism in peripheral blood (mean VEH 40.7% vs. RUX 37.7% vs. TAM 17.3%, $p \leq 0.0059$) of *Jak2*^{V617F}-deleted mice versus ruxolitinib treated mice **(Figure 3E-F, Supp. Figure 8B-D)**. Reductions in total erythroid progenitors were observed with both ruxolitinib and TAM treated mice by the conclusion of the study (mean VEH 0.55×10^6/mL vs. RUX 0.28×10^6/mL vs. TAM 0.21×10^6/mL, $p \leq 0.001$), with a greater effect on megakaryocytic progenitor (mean VEH 0.55×10^6/mL vs. RUX 0.53×10^6/mL vs. TAM 0.23×10^6/mL, $p \leq 0.05$) and total megakaryocyte output with *Jak2*^{VF} deletion specifically **(Supp. Figure 8E-H)**. Most importantly, the reduction in mutant cell fraction seen with *Jak2*^{V617F} deletion within hematopoietic progenitor (GMP: $p \leq 0.0001$, MEP: $p \leq 0.0001$) and LSK stem cell enriched populations was not observed with pharmacologic type I JAK inhibition (mean VEH 87.9% vs. RUX 87.6% vs. TAM 28.7%, $p \leq 0.0001$) **(Figure 3G)**.

We previously showed that the type II JAK2 inhibitor CHZ868 showed improved efficacy compared to ruxolitinib *in vivo*.(34) Consistent with these observations, treatment with CHZ868 showed greater efficacy than ruxolitinib in regard to improvement in hematologic parameters (mean Hct: CHZ868 50.3% vs. RUX 85.8%, $p \leq 0.0001$) and spleen volume reduction (mean CHZ868 76 mg vs. RUX 235 mg, $p < 0.0001$), on par with *Jak2*^{V617F} deletion **(Figure 3E-F, Supp. Figure 8B-C)**. Significant reductions in MEP, GMP, and LSK mutant allele burden, as well as in more committed MEP populations, were also observed in CHZ868 treated mice compared to VEH/ruxolitinib-treated mice (LSK: $p \leq 0.02$, GMP: $p \leq 0.013$, MEP: $p \leq 0.013$), but not to the extent seen with *Jak2*^{V617F} deletion **(Figure 3G, Supp. Figure 8F-G)**. These data

confirm that more potent, selective target inhibition, including with type II JAK inhibitors, offers the potential for greater therapeutic efficacy when compared to current type I JAK inhibitors.

Previous studies have suggested that MAPK signaling plays an important role in MPN disease cell survival in the setting of type I JAK inhibitor therapy,(13) and recent work has implicated the MAPK-dependent factor YBX1 as a critical mediator of *JAK2*^{V617F}-mutant cell persistence.(14) We observed distinct effects on MAPK activity by RNA-Seq with ruxolitinib treatment vs. *Jak2*^{V617F} deletion in comparison to VEH treated mice. Negative regulators of KRAS signaling were down-regulated with ruxolitinib (NES -1.64, *FDR* $\leq$ 0.0005) and up-regulated with *Jak2*^{V617F} deletion (NES 1.35, *FDR* $\leq$ 0.039) in MEPs suggesting enhanced MAPK signaling with ruxolitinib and MAPK attenuation with *Jak2*^{V617F} deletion **(Figure 3H)**. Immunohistochemistry of bone marrow sections confirmed increased phospho-ERK abundance in ruxolitinib-treated mice that was abrogated with *Jak2*^{V617F} deletion **(Figure 3I)**, and genotype-specific scATAC-Seq revealed increased accessibility of MAPK-mediated AP-1 factors FOS/JUN(35) within HSPCs of ruxolitinib-treated MF patients in comparison to untreated MF HSPCs consistent with enhanced MAPK activity **(Supp. Figure 8I)**. Furthermore, expression of *Ybx1* in sorted murine cKit^{+} cells was increased with ruxolitinib therapy but potently suppressed with *Jak2*^{V617F} deletion (mean rel. exp. VEH 1.37 vs. RUX 2.52 vs. TAM 0.42, $p \leq 0.0094$) **(Figure 3J)**. These data suggest that potent, mutant-specific *Jak2*^{V617F} targeting can abrogate pathologic MAPK signaling and Ybx1-mediated persistence of *Jak2*^{V617F}-mutant HSPCs.

JAK2^{V617F} dependency with cooperative TET2 loss

Previous studies of mutational order in primary MPN cells have shown that cooperating mutations in epigenetic regulators, including TET2, can precede the acquisition of JAK2^{V617F} in the clonal evolution of MPN and that antecedent TET2 mutations can alter the *in vitro* sensitivity to ruxolitinib.(36) In addition, TET2 loss is the most frequently co-occurring mutation with JAK2^{V617F} in MPNs, and *in vitro* and *in vivo* studies have shown that concurrent TET2 and JAK2^{V617F} mutations promote enhanced mutant HSC fitness and increased risk of MPN disease progression.(37-39) Our *Jak2*^{RL} system allows for the assessment of JAK2^{V617F} dependency in the setting of co-occurring mutant allele activation/inactivation, including in the context of antecedent mutations in epigenetic regulators. We therefore assessed the impact of *Jak2*^{V617F} activation in concert with pre-existing *Tet2* loss with the reversible *Jak2*^{RL} allele **(Figure 4A)**. Mice transplanted with *Dre*-electroporated *Ubc:CreER-Jak2*^{RL}*/Tet2*$^{-/-}$ cells demonstrated

enhanced leukocytosis (mean 13.1 K/μL vs. 26.0 K/μL, $p \leq 0.001$) and thrombocytosis, increased spleen volumes (mean 317.6 mg vs. 612.2 mg, $p \leq 0.021$), and expanded mutant peripheral blood chimerism (mean 25.9% vs. 39.9%, $p \leq 0.025$) compared to *Ubc:CreER-Jak2*^{RL} and single-mutant *Tet2*$^{-/-}$ transplanted mice **(Figure 4B-D, Supp. Figure 9A)**. *Tet2*$^{-/-}$ and *Jak2*^{RL}*/Tet2*$^{-/-}$ HSCs also exhibited improved serial replating capacity in colony forming assays compared to single-mutant *Jak2*^{RL} cells **(Supp. Figure 9B)**. *Ex vivo* co-culture of *Tet2*$^{-/-}$ and *Jak2*^{RL}*/Tet2*$^{-/-}$ cells over BMECs exhibited a near 3-fold increase in hematopoietic cell output (mean 2.92 × 10^6/mL vs. 2.41 × 10^6/mL vs. 0.80 × 10^6/mL, $p \leq 0.005$), including among Mac1$^+$ mature myeloid cells (mean 1.04 × 10^6/mL vs. 0.60 × 10^6/mL vs. 0.22 × 10^6/mL, $p \leq 0.023$), compared to *Jak2*^{RL} cells consistent with the known role of TET2 loss-of-function in enhancing myeloid lineage commitment **(Supp. Figure 9C)**.(40) Together, these data are phenotypically consistent with previous *Tet2*$^{-/-}$ and *Jak2*^{VF}*/Tet2*$^{-/-}$ models(37,38) and highlight the utility of the Dre-Cre dual recombinase system to model sequential acquisition of mutations *in vivo* and mimic the evolution of disease from a pre-malignant, clonally restricted hematopoietic state (i.e. single-mutant *Tet2*$^{-/-}$ knock-out) to overt MPN.

We next evaluated effects of *Jak2*^{V617F} deletion on *Jak2*^{RL}*/Tet2*$^{-/-}$ mutant cell fitness *in vivo* in competition with Cd45.1 bone marrow. Treatment with TAM at 9 weeks post-transplant resulted in normalization of hematologic parameters ($p \leq 0.005$) and reductions in peripheral blood mutant cell fraction of double-mutant cells to a similar extent observed with *Jak2*^{V617F} deletion in single-mutant *Jak2*^{RL} transplanted mice **(Figure 4E-F)**. Further, spleen sizes (mean 103 mg vs. 529 mg, $p \leq 0.0001$) and total BM cellularity (femur; mean 11.6 × 10^6/mL vs. 15.7 × 10^6/mL, $p \leq 0.0035$) were similarly normalized with *Jak2*^{V617F} deletion **(Supp. Figure 9D-E)**. While the extent of reticulin fibrosis was increased in *Jak2*^{RL}*/Tet2*$^{-/-}$ mice compared to *Jak2*^{RL}, mutant allele reversal resolved fibrosis in both mutational contexts **(Figure 4G)**. The reduction in mutant cell fraction, as was observed with single-mutant mice, persisted down to the level of HSPCs in TAM-treated *Jak2*^{RL}*/Tet2*$^{-/-}$ mice, including within the LSK stem cell-enriched compartment (mean TAM 28.7% vs. MPN 73.7%, $p \leq 0.001$) **(Figure 4H, Supp. Figure 9F)**. This decrease in mutant cell fraction appeared, at least in part, to be due to increased apoptosis, as *ex vivo* treatment with 4-OHT resulted in an increase in Annexin V+ cells in *Jak2*^{RL} and double-mutant cells, but not Tet2$^{-/-}$ cells **(Supp. Figure 9G)**. This effect was specific to *Jak2*^{V617F} deletion, as treatment of *Tet2*$^{-/-}$ and *Jak2*^{RL}*/Tet2*$^{-/-}$ mice with type I JAK inhibition (ruxolitinib) did not alter allelic fraction **(Supp. Figure 9H)**. Finally, in a subset of assayed *Jak2*^{RL}*/Tet2*$^{-/-}$ mice following *Jak2*^{V617F} deletion (4/9), we were unable to detect *Tet2*$^{-/-}$ knock-out bands in whole marrow at

time of sacrifice. Cells harvested from *Jak2*^{RL}/*Tet2*$^{-/-}$ recipient mice following oncogenic deletion were unable to serially replate indicating loss of self-renewal capacity in comparison to control double-mutant mice **(Figure 4I, Supp. Figure 9I)**. These data support the notion that co-occurring loss-of-function mutations of TET2 do not dramatically alter reliance on JAK/STAT signaling for disease maintenance, and that despite the fitness advantage engendered by TET2 loss on MPN HSCs, the reductions in HSC fitness in the setting of *Jak2*^{V617F} reversion suggest a unique dependency on oncogenic JAK2^{V617F} that renders double-mutant cells susceptible to eradication.

DISCUSSION

Mutated kinases occur frequently in cancer and are amenable to targeted inhibition; however, mechanisms mediating acquired resistance have been observed for most targeted therapies.(41) By contrast, current JAK inhibitors fail to eliminate JAK2^{V617F}-mutant clones in MPN patients suggesting inadequate target inhibition and/or other genetic/non-genetic factors mediate JAK2^{V617F}-mutant cell persistence in the setting of JAK inhibitor therapy.(42) We show in preclinical models that there is an absolute requirement for JAK2^{V617F} in MPN cells and that mutant-specific targeting of JAK2^{V617F} abrogates MPN features, reduces mutant cell fraction, and extends overall survival with concomitant depletion of disease-sustaining stem cells within the HSPC compartment. Further, our data suggest that JAK2^{V617F} dependency persists even in the setting of antecedent mutations in epigenetic regulators, specifically TET2. Moreover, we demonstrate the feasibility of our dual-recombinase system to evaluate oncogenic signaling dependencies *in vivo*, and we believe that a similar approach will allow us to assess oncogenic dependencies and mechanisms of mutant-mediated transformation across a spectrum of malignant contexts.

These data support the notion that improved targeting of aberrant JAK2 signaling and downstream effectors offers greater therapeutic potential than current JAK kinase inhibitors and that JAK2^{V617F} mutant-selective inhibition represents a potential curative strategy for the treatment of MPN patients. Clinical translation may include more potent JAK kinase inhibitors which inhibit both mutant and WT JAK2, as shown preclinically with the type II JAK inhibitor CHZ868 in MPN models and in B-cell acute lymphoid leukemia (ALL).(34,43) Recent data highlight the potential for selective targeting of mutant calreticulin (CALR) in MPNs,(44) and the elucidation of the first full length mutant JAK kinase structure(45) provides a path to the

development of true mutant-specific JAK2^{V617F} inhibitors. As more potent (type II JAK2 inhibitors) and mutant selective JAK2^{V617F} inhibitors enter the clinic, we expect that these agents will show increased efficacy, including the ability to substantively reduce mutant allele burden. Our studies suggest that therapeutic agents which more potently inhibit constitutive JAK2 signaling will offer greater benefit to MPN patents than current therapies, including in the presence of cooperating clonal hematopoesis disease alleles.

MATERIALS AND METHODS

Experimental animals All animal studies were performed in accordance with institutional guidelines established by Memorial Sloan Kettering Cancer Center (MSKCC) under the Institutional Animal Care and Use Committee-approved animal protocol (#07-10-016) and the Guide for the Care and Use of Laboratory Animals (National Academy of Sciences 1996). All experimental animals were maintained on a 12 hour light-dark cycle with access to water and standard chow ad libitum. Veterinary staff provided regular monitoring and husbandry care. All mice had intact immune systems, were drug and test naïve, and had not been involved in previous procedures. Animals were monitored daily for signs of disease or morbidity, bleeding, failure to thrive, infection, or fatigue and sacrificed immediately if they exhibited any signs of the above. Mice harboring the *Jak2*^{RL} allele were generated by Ingenious Targeting Laboratory (Ronkonoma, NY) in a C57BL/6J background. Specifically, a 8.86kb genomic DNA used to construct the targeting vector was first subcloned from a positively identified C57BL/6J BAC clone (RP23-316C6). The region was designed such that the long homology arm (LA) extends ~6 kb 5' to the cluster of Lox2272-Rox-Rox12-Lox2272 sites, and the short homology arm (SA) extends about 2.2 kb 3' to the Neo cassette and 3' Rox12 site. The inversion cassette is in between the second set of Lox2272 and Rox sites, and it consists of the mutant exon 14* (V617F) and its flanking genomic sequences for correct splicing (SaE14*Sd). The inversion cassette replaces WT exon 14 and the same flanking genomic sequences included in the cassette. The BAC was sub-cloned into a ~2.4kb pSP72 (Promega) backbone vector containing an ampicillin selection cassette for retransformation of the construct. Ten micrograms of the targeting vector was then linearized and transfected by electroporation of FLP C57BL/6J (B6) embryonic stem cells. After selection with G418 antibiotic, surviving clones were expanded for PCR analysis to identify recombinant ES clones. After successful clone identification, the neomycin cassette was removed with a transient pulse of Cre recombinase and clones were reconfirmed following expansion. Finally, ES cells were injected in C57BL/6J mice via tetraploid

complementation (NYU). *Tet2*$^{f/f}$ conditional knock-out mice, Cre-*lox* *Jak2*^{V617F} knock-in mice, RC::RLTG reporter mice, Cre TdTomato reporter mice, and *Ubc:CreER* mice have been described previously.(2,21,24,40,46) 6-8 week old female and male *Jak2*^{RL} or *Jak2*^{RL}/*Tet2*$^{f/f}$ donor mice were used for Dre electroporation knock-in experiments. Age-matched 6-10 week old female mice were used as donors for all transplant experiments (Ly5.1 Cd45.1 competitive or C57BL/6J non-competitive). All Jak2^{RL} donor mice used were crossed in a heterozygous fashion so as to retain a WT copy of JAK2.

Mouse genotyping DNA was isolated using the DNeasy Blood & Tissue Kit (Qiagen, Germantown, MD). The presence of the *Jak2*^{RL} locus was genotyped using the following primers: FWD:5'-CGTGCATAGTGTCTGTGGAAGTC-3'; REV: 5'-CGTGGAGAGTCTGTAAGGCTCAA-3'. The WT allele gives a band of 246bp; the mutant allele gives a band of 833bp. *Jak2*^{V617F} knock-in genotyping was carried out with the following primers: FWD: 5'-GCCATCTTTCCAGCCTAAAATTAG-3'; REV: 5'-TCCAAAGAGTCTGTAAGTACAGAACT-3' and with the following reaction conditions: 94°C for 3 minutes followed by 15 cycles of 94°C for 15s, 65°C for 15s, and 72°C for 30s decreasing by 1°C per cycle, and then followed by an additional 25 cycles of 94°C for 15s, 50°C for 15s, and 72°C for 30s. *Jak2*^{V617F} knock-out genotyping was carried out using the following primers: FWD: 5'-GCCATCTTTCCAGCCTAAAATTAG-3'; REV: 5'-ACCAGTTGCTCCAGGGTTACACG-3' and with the following reaction conditions: 94°C for 2 minutes followed by 30 cycles of 94°C for 30s, 53°C for 30s, and 72°C for 30s. Sequencing of the unrecombined Rox-lox locus was carried out using the following primers: FWD: 5'-AGGAGCATCGATGACTACATGATGAG-3'; REV: 5'-AGACTCTCCACGGTCTCATCTACG-3' and with the following reaction conditions: 98°C for 30 seconds followed by 35 cycles of 98°C for 10s, 65°C for 15s, and 72°C for 30s. *Tet2* genotyping were carried out using the following primers/conditions: FWD: 5'-AAGAATTGCTACAGGCCTGC-3'; REV: 5'-TTCTTTAGCCCTTGCTGAGC-3'; ExR: 5'-TAGAGGGAGGGGGCATAAGT-3' and with the following reaction conditions: 94°C for 2 minutes followed by 39 cycles of 94°C for 35s, 58°C for 45s, and 72°C for 55s. Annotation of PCR genotyping results was carried out on a QIAxcel Advanced System (Qiagen) and analyzed using QIAxcel ScreenGel software (Qiagen). Sanger sequencing was performed by Genewiz (South Plainfield, NJ) and analyzed using Benchling software.

Dre mRNA electroporation *Dre* mRNA was purchased from TriLink Biotechnologies (San Diego, CA) and electroporation carried out using the Neon Transfection System

(ThermoScientific) per the manufacturer's protocol. Specifically, bone marrow donor cells were isolated from limb bones into phosphate buffered saline (PBS; pH 7.2) containing 2% fetal calf serum via centrifugation. After red blood cell (RBC) lysis, single-cell suspensions were depleted of lineage-committed hematopoietic cells using a Lineage Cell Depletion Kit according to manufacturer's protocol (EasySep™, StemCell Technologies, Inc.). 2.5-3.0 × 10^6 lineage-depleted bone marrow was then washed in PBS and then resuspended in 135 µL Buffer T to which 15 µL of *Dre* mRNA (at 1 µg/µL) was quickly added and electroporated at the following conditions: 1700V for 20ms x1 pulse. The cells were then pipetted into penicillin-streptomycin free StemSpan SFEM medium with thrombopoietin (TPO; 20 ng/mL; PeproTech) and stem cell factor (SCF; 20 ng/mL; PeproTech), cultured for two hours, and then subsequently harvested and washed/resuspended in PBS and transplanted via lateral tail vein injection into lethally irradiated (900cGy) 6-8 week old C57BL/6J recipient mice at approximately 4 × 10^5 cells per recipient along with 50,000 un-electroporated WT whole bone marrow support cells. Single-mutant $Tet2^{-/-}$ or double-mutant $Jak2^{RL}/Tet2^{-/-}$ transplants/electroporations were carried out as above, except donor mice were dosed with TAM (100 mg/kg by oral gavage daily x4; purchased from MedChemExpress) 6-8 weeks prior to harvest and excision confirmed prior to *Dre* electroporation.

Transplantation assays and* in vivo *experiments $Jak2^{RL}$, $Tet2^{f/f}$, and $Jak2^{RL}/Tet2^{f/f}$ lines were crossed to *Ubc:CreER* TAM-inducible Cre lines and RLTG dual-recombinase reporter lines.(24,46) Primary recipient mice transplanted with *Dre* mRNA-recombined *Ubc:CreER-*$Jak2^{RL}$, *Ubc:CreER-*$Tet2^{-/-}$, or *Ubc:CreER-*$Jak2^{RL}/Tet2^{-/-}$ bone marrow cells were bled every 3-4 weeks post-transplant to monitor disease status. Peripheral blood was isolated by submandibular bleeds and complete blood counts determined using a ProCyte Dx (IDEXX Laboratories, Westbrook, ME) per manufacturer's instruction. For competitive repopulation assays, 1.2 × 10^6 whole bone marrow from primary transplant recipient mice exhibiting MPN was harvested 6-8 weeks post-transplant and combined with age-matched 0.8 × 10^6 Cd45.1 (Jackson Laboratories, Bar Harbor, ME) whole bone marrow and transplanted into 6-8 week old lethally irradiated Cd45.1 secondary recipient mice. Mice transplanted with Dre-recombined $Jak2^{V617F}$ cells demonstrating low Cd45.2 chimerism at baseline (<15%) and/or evidence of poor MPN cell engraftment were excluded from study cohorts. To induce Cre and delete $Jak2^{V617F}$, mice were treated with TAM (purchased from MedChemExpress) 100 mg/kg daily (dissolved in corn oil) by oral gavage x 4 followed by 14 days of TAM chow (80 mg/kg daily; ENVIGO). Tamoxifen control studies were carried out using similar dosing schedules on 45.1 mice

transplanted in competition with *Dre*-electroporated, Cre-negative *Jak2*^{RL} MPN bone marrow cells. For terminal tissue isolation, mice were euthanized with CO_2 asphyxiation, and tissues were dissected and fixed with 4% paraformaldehyde for histopathological analysis. For whole bone marrow isolation, the femurs, hips, and tibias were dissected and cleaned. Cells were then isolated using centrifugation at 8000xG for 1 minute followed by RBC lysis (BioLegend) for 10-15 minutes. Bone marrow cell numbers and viability were determined using an automated cell counter (ViCell Blu, Beckman Coulter). Spleen cell suspensions were generated by crushing whole spleen and filtering through a 70 μM filter. RBC lysis (BioLegend) was performed and cells were prepared for downstream processing or frozen.

In vivo *drug studies* For *in vivo* inhibitor studies, approximately 8 weeks following transplant, secondary transplant cohorts of lethally-irradiated mice transplanted with *Ubc:CreER-Jak2*^{RL} bone marrow in competition with Cd45.1 marrow (as above) and exhibiting active MPN were bled and cohorted based on peripheral blood Cd45.2 chimerism and total WBC count to achieve congruency across treatment arms. Mice were then treated with ruxolitinib (60 mg/kg P.O. twice daily; dissolved in 20% Captisol in PBS; purchased from MedChemExpress), CHZ868 (30 mg/kg P.O. daily; dissolved in 0.5% methylcellulose + 0.5% Tween-80 in dH_2O; purchased from MedChemExpress), TAM to delete *Jak2*^{V617F} (as above; purchased from MedChemExpress), or VEH. Investigators were not blinded to the identity of mice or samples. Mice were treated for a total of 6 weeks before timed sacrifice and marrow/spleen harvested as above.

Bone marrow endothelial cell (BMEC) culture Bone marrow cells were isolated from limb bones into FACS buffer (phosphate buffered saline [PBS] + 2% fetal bovine serum) via centrifugation. After RBC lysis, single-cell suspensions were depleted of lineage-committed hematopoietic cells using a Lineage Cell Depletion Kit according to manufacturer's protocol (EasySep™, StemCell Technologies, Inc.). Subsequently, 50,000 of the resulting lineage$^-$ cells were plated on a confluent monolayer of BMECs in a single well of a 12-well plate. Each well had 1 mL StemSpan SFEM (StemCell Technologies, Inc.) with 20 ng/mL recombinant murine SCF (PeproTech) in addition to the corresponding drug treatment: either 4-hydroxytamoxifen (4-OHT; Sigma Aldrich; stock concentration: 13 mM) or its VEH, appropriately diluted in media to its final concentration (i.e., 0.01% (v/v) of ethanol (EtOH), or 200 nM, 400 nM or 1 μM of 4-OHT) (three replicates/condition). The BMECs were seeded two days before plating the lineage$^-$ cells at a density of 100,000 cells/well. Co-cultures were maintained for a total of 7 days at 37°C and 5% CO_2, with media being completely refreshed with the original SCF and drug/VEH

concentrations. 4-OHT or EtOH VEH was added to the culture on day 1 and again on day 4. On day 7, total cells were harvested with Accutase (Biolegend) and cell numbers were determined via an automatic cell counter (ViCell Blu, Beckman Coulter). Cells were then stained with the desired antibody cocktail and phenotyped by flow cytometry.

Flow cytometry, cell sorting, and western blot Following single cell preparation, murine peripheral blood, whole bone marrow, or spleen mononuclear cells were lysed for 10-15 minutes with RBC lysis buffer (BioLegend, San Diego, CA) and washed twice with FACS buffer. Cells were then resuspended in Fc (Cd16/32) block for 15 minutes and then subsequently stained with a cocktail comprised of antibodies targeting Cd3 (17A2), Cd45R/B220 (RA3-6B2), Gr-1 (RB6-8C5), Cd11b (M1/70), Cd45.2 (104), and Cd45.1 (A20) for 30 minutes. For hematopoietic stem/progenitor cell analysis, lysed bone marrow was stained with a cocktail of lineage markers along with antibodies against cKit (2B8), Sca1 (D7), FcγRII/III (2.4G2), Cd34 (RAM34), Cd150 (9D1), and Cd48 (HM48-1). Erythroid progenitor flow was carried out on unlysed bone marrow or spleen with the addition of the following antibodies: Cd105 (43A3), Cd71 (R17217), Cd41 (MWReg30), and Ter119 (Ter-119). All FACS antibodies were purchased from BD, BioLegend, or eBioscience. Following antibody incubation, cells were washed with FACS buffer and resuspended in a DAPI-containing FACS buffer solution for analysis and sorting. Samples were run on a LSRFortessa (Becton Dickinson) using FACSDiva software and analyzed with FlowJo v10.8.1 (Treestar, Ashland, OR, USA). For sorting of Cd45.2+ lin^- $Sca1^+cKit^+$ experiments, whole bone marrow samples were stained with antibodies for lineage cocktail, cKit, Sca1, as well as Cd45.2 and Cd45.1 as above, and gated and sorted on Lin^- $cKit^+Sca1^+$ $Cd45.2^+$ fractions using a FACSAria 3 (Becton Dickinson) instrument. Samples were subsequently spun at 1500 rpm for 5 minutes, resuspended in Buffer ATL Cell Lysis solution (Qiagen) and DNA extracted using the DNA Micro Kit (Qiagen) per the manufacturer's instructions. For Western blot analysis, whole-cell protein extracts from harvested splenocytes were prepared using RIPA buffer (ThermoScientific, Rockford, IL) containing a protease/phosphatase inhibitor cocktail (Thermo Scientific). Protein quantification was performed using the Pierce BCA protein assay kit (ThermoScientific) and analyzed on a Cytation 3 plate reader (BioTek). Proteins were separated by NuPAGE 4-12% Bis-Tris Gel and transferred to a nitrocellulose membrane. The following antibodies were used: β-actin (Cell Signaling 4970S), STAT5 (Cell Signaling 94205S), and pSTAT5 (Cell Signaling, 9359S). Images were obtained using the ChemiDoc Imaging System (BioRad) and analyzed using ImageLab software (BioRad).

Histology staining and immunohistochemistry (IHC), and photography Tibia and spleen samples were fixed in 4% paraformaldehyde for over 24 hours and then embedded in paraffin. Paraffin sections were cut on a rotary microtome (Mikrom International AG), mounted on microscope slides (ThermoScientific), and air-dried in an oven at 37°C overnight. After drying, tissue section slides were processed either automatically for hematoxylin and eosin (H&E) staining (COT20 stainer, Medite), or manually for reticulin staining. All samples and slide preparation, including immunohistochemistry was carried out at the Tri-Institutional Laboratory of Comparative Pathology (LCP) core facility. The following antibodies were used for immunohistochemistry: Mac1 (Cedarlane CL8941B, 1:100), Ter119 (BDBioscience, 550565 1:200), and p-44/42 MAPK (Erk1/2) (Cell Signaling 4376, 1:100). Pictures were taken at 100X, 200X and 400X (H&E, reticulin and respective IHC) magnification using an Olympus microscope and analyzed with Olympus Cellsens software. Tissue sections were formally evaluated by a hematopathologist (W. Xiao), including reticulin scoring.

Assessment of cell cycle, apoptosis, and viability Apoptosis was measured by flow cytometry on a LSRFortessa (Becton Dickinson) cytometer with Annexin V PerCPCy5.5 antibody (BioLegend) in combination with the antibody cocktail (above) in Annexin binding buffer (BioLegend) at 1:50 dilution in combination with DAPI as live/dead cell stain. For cell cycle analysis, lineage-negative marrow was surface stained with the LSK antibody cocktail above followed by the Zombie UV Fixable Viability Kit (BioLegend), and then subsequently fixed and permeabilized using the FIX&PERM Cell Permeabilization Kit (Invitrogen) per manufacturer's instructions and stored at -20C until further staining. Cells were then washed twice in FACS buffer, pelleted and stained with anti-Ki67 antibody (BioLegend) or isotype control for 30 minutes, washed again and resuspended in FACS buffer with DAPI. Samples were run on linear for DAPI stain.

Colony forming assays To assess colony formation and serial replating capacity, RBC-lysed 50,000 whole bone marrow cells were seeded in 1.5mL MethoCult M3434 (Stem Cell Technologies) with no additional supplemental cytokines in triplicate on 6 well plates and scored on day 8. For replating, cells were harvested and pooled and then re-seeded once more at 50,000 cells/well in 1.5mL MethoCult M3434 in triplicate. We assessed *Dre* mRNA-mediated recombination efficiency both pre- and post-transplant using either freshly *Dre*-electroporated *Jak2*^{RL} lineage-negative bone marrow cells, or whole marrow harvested 6 weeks following

transplant from primary recipient mice transplanted with *Dre*-electroporated *Jak2*^{VF} knock-in marrow. These cells were seeded as above and after 7 days, individual colonies plucked into 70μL of Buffer ATL and DNA extraction carried out using the DNA Micro Kit (Qiagen) per the manufacturer's instructions.

Serum cytokine profiling Serum samples were diluted two-fold with PBS (pH 7.2) and stored at -80°C until analysis. Cytokine assays were carried out using the Millipore Mouse Cytokine 32-plex kit and FlexMAP 3D platform (Luminex) per the manufacturer's instructions. xPONENT (Luminex) and Milliplex Analyst Software (Millipore) was used to convert mean fluorescent intensities (MFI) values into molecular concentrations using a standard curve (5-parameter logistic fitting method). Data were then normalized by first transforming concentration values using the log2 function and the mean and standard deviation (SD) of the log values calculated across all samples for each analyte. Z-scores were then computed using the formula Z-score = (Mean of log2 concentration values for an analyte per condition – mean of average log2 values for an analyte across all conditions)/SD, calculated across the three conditions (WT, MPN, TAM), and then used to normalize the cytokine data. The heatmap was generated using the R package tidy_heatmap to visualize Z-score normalization for cytokines that displayed differential expression across the groups.

RNA sequencing (RNA-Seq) and data analysis For gene expression analysis, secondary cohorts of lethally irradiated C57BL/6J mice transplanted with *Ubc:CreER-Jak2*^{RL}-RLTG reporter bone marrow 8 weeks post-transplant and exhibiting MPN were treated with ruxolitinib (60mg/kg P.O. twice daily), TAM (100mg/kg by oral gavage daily × 4 followed by 80mg/kg of TAM chow × 3 days) +/- VEH (MPN control) for 7 days and then sacrificed. Lineage-depleted bone marrow was isolated and stained with an antibody cocktail containing a combination of lineage markers along with antibodies against cKit (2B8), Sca1 (D7), FcγRII/III (2.4G2), and Cd34 (RAM34) for 30 minutes, washed, and then resuspended in FACS buffer containing DAPI as a live/dead stain. TdTomato+ (*Jak2*^{RL} knock-in) or GFP+ (*Jak2*^{RL} knock-out) LSKs and MEPs were then sorted on a FACSAria III directly into Trizol LS (Invitrogen) and stored at -80°C until processing. RNA was subsequently isolated using the Direct-Zol Microprep Kit (Zymo Research, R2061) according to manufacturer's protocol and quantified using the Agilent High Sensitivity RNA ScreenTape (Agilent 5067-5579) on an Agilent 2200 TapeStation. cDNA was generated from 1 ng of input RNA using the SMART-Seq HT Kit (Takara 634455) at half reaction volume followed by Nextera XT (Illumina FC-131-1024) library preparation. cDNA and tagmented libraries were

quantified using High Sensitivity D5000 ScreenTape (5067- 5592) and High Sensitivity D1000 ScreenTape respectively (5067- 5584). Libraries were sequenced on a NovaSeq at the Integrated Genomics Operation (IGO) at MSKCC. FASTQ files were mapped and transcript counts were enumerated using STAR (genome version mm10 and transcript version M13). Counts were input into R and RNA-Sequencing analysis using DESeq2. Genes were filtered out prior to modeling in DESeq if they were not detected in all, with MEPs and LSKs modeled separately. Differentially expressed genes were identified with a log2-foldchange of 1 and an adjusted *p* value of 0.05. Gene set enrichment analysis was performed using the fgsea package at 100,000 permutations with genesets extracted from the msigdbr package. Single sample gene set enrichment analysis was performed using the gsva package. To determine the frequency of the *Jak2*^{V617F} allele and relative mutant expression, the samtools(v1.5)/mpileup variant calling tool was used. A minimum mapping quality of 30 for each read and default minimum base quality of 13 was used. Maximum depth was set to 100,000. Bcftools (v1.8) was used to convert BCF files into VCF files, and the vcfR (v1.14) package in R was used to parse the VCF files of alternative and reference alleles and read depth counts. Statistical differences between the different conditions were calculated using the one-sided wilcoxon rank sum test. Figures were prepared using the ggplot2, ggsignif, ggrepel, and tidyheatmaps packages in R. Complete scripts can be found on github at https://github.com/bowmanr/goldilox.

Mouse Assay for Transposase-Accessible Chromatin Sequencing (ATAC-Seq) and data analysis Chromatin accessibility assays utilizing the bacterial Tn5 transposase were performed as described.(47) Briefly, 5.0 × 10^4 TdTomato+ (*Jak2*^{RL} knock-in) or GFP+ (*Jak2*^{RL} knock-out) cKit$^+$ bone marrow cells from mice treated for 7 days with TAM or an untreated MPN control cohort were sorted on a FACSAria III directly into PBS and subsequently lysed and incubated with transposition reaction mix containing PBS, Tagment DNA buffer, 1% Digitonin, 10% Tween-20, and Transposase (Illumina). Samples were then incubated for 30 minutes at 37°C in a thermomixer at 1000 rpm. Prior to amplification, samples were concentrated with the DNA Clean and Concentrator Kit-5 (Zymo). Samples were eluted in 20 µL of elution buffer and PCR-amplified using the NEBNext 2X Master Mix (NEB) for 11 cycles and sequenced on a NextSeq 500 (Illumina). All samples were processed at the Center for Epigenetics Research (CER) core facility at MSKCC. Libraries were sequenced on a NovaSeq at the Integrated Genomics Operation (IGO) at MSKCC. Data analysis was completed through in house scripts at the CER, in brief: reads were trimmed with 'trim_galore' and aligned to mouse genome mm9 using bowtie2 (default parameters). Duplicates were removed with the Picard tool 'MarkDuplicates',

and peaks were called with MACS2, merged and used to create a full peak atlas. Read counts were tabulated over this atlas using featureCounts. Downstream differential enrichment testing was completed in DESeq2 with default normalization scheme. HOMER was used for known motif enrichment amongst the differentially enriched peaks as defined by a fold change of +/- 1.5 and an adjusted *p* value of 0.1. For the lineage deconvolution analysis presented in Supplemental Figure 6H, we performed a process which uses a reference library from aggregated biological replicates across multiple cell types and selecting key lineage-specific loci to deconvolve samples and generate component estimates.(30) A non-negative least squares regression (NNLS) comparing each unknown sample to the set of normal hematopoietic states is then performed. Deconvolution coefficients are interpreted as proportions to estimate the magnitude per hematopoietic stage.

Human single-cell ATAC-Seq and data analysis Single-cell ATAC-Seq data was processed using cellranger-ATAC (v2.0.0) mkfastq. ATAC sequencing reads were then aligned to the hg38 reference genome using cellranger-ATAC count function. Fragment files generated by cellranger-ATAC were used as input for the ArchR(48) (v1.0.0). For initial dimensionality reduction and patient data integration, the cell by genomic bin matrix was used as input for reciprocal latent semantic indexing (LSI) as calculated by the Signac (v1.1.1). Transcription factor motif accessibility z-scores were calculated with ChromVAR(49) (v1.8.0). The earliest HSPCs (cluster HSPC1, see Myers, R. and Izzo, F. *et al*., *Nature, in press*, 2024) were subset for downstream analysis, and statistical comparisons of motif accessibility for NFKB1, REL, FOS, and JUN transcription factors were performed via linear mixture model including patient identity as random effect to account for potential technical confounders arising from sample-specific batch effects. For heatmap representation, motif accessibility z-scores were used as input and the pheatmap (v1.0.12) R package was used.

Quantitative real-time PCR Total RNA was extracted from magnetic-bead isolated cKit$^+$ bone marrow (Miltenyi Biotec) using the Direct-zol RNA extraction kit (Zymo) per manufacturers' protocols respectively. Complementary DNA was then reverse transcribed using the Verso cDNA Synthesis kit (ThermoFisher Scientific). *Ybx1* expression was evaluated by quantitative reverse-transcription (qRT) PCR using Taqman probes purchased from ThermoFisher (Mm00850878_g1) on the RealPlex thermocycler (ThermoFisher Scientific, Fairlawn, NJ).

Statistical analysis Statistical analyses were performed using Student's *t*-test (normal distribution) using GraphPad Prism version 6.0h (GraphPad Software, San Diego, CA) unless otherwise noted. Kaplan-Meier curves were determined using the log-rank test. $P<0.05$ was considered statistically significant. For the cytokine analysis presented in Figure 1F and Supplemental Figure 3J, individual cytokines were analyzed using the Kruskal-Wallis test with lower values set at the lower limit of the assay and *p* values generated by doing multiple comparisons testing across treatment arms (WT vs. MPN vs. TAM) and adjusting based on False Discovery Rate (FDR) of $\leq$ 0.05. The number of animals, cells and experimental replication can be found in the respective figure legends.

Data availability Raw and processed sequencing data is made available at https://github.com/bowmanr/goldilox and via the NCBI Gene-Expression Omnibus (GEO) at GSE203464.

ACKNOWLEDGEMENTS

We are grateful to members of the Levine Lab for their discussion of the work. We would also like to acknowledge Dr. Alex Joyner (MSKCC), Dr. Patricia Jensen (NIH) and Dr. Tudor Badea (NIH) for discussion on Dre-Rox technology, and to Sime Brkic (University Hospital Basel Switzerland) for their technical advice and support. This work was supported by the National Cancer Institute award P01 CA108671 (R.L.L.). R.L.L. was supported by a Leukemia and Lymphoma Society Scholar award. A.J.D. is a William Raveis Charitable Fund Physician-Scientist of the Damon Runyon Cancer Research Foundation (PST-24-19). He also has received funding from the National Institute of Health (T32CA009207), American Association of Cancer Research (17-40-11-DUNB) and the American Association of Clinical Oncology. R.L.B. was supported by a Damon Runyon-Sohn Fellowship and the National Cancer Institute (K99CA248460). R.M.M. is supported by a Medical Scientist Training Program grant from the National Institute of General Medical Sciences of the National Institutes of Health under award number T32GM007739 to the Weill Cornell/Rockefeller/Sloan Kettering Tri-Institutional MD-PhD Program and by the Weill Cornell Medicine NYSTEM Training Program under award number C32558GG. F.I. is supported by the American Society of Hematology Fellow-to-Faculty Scholar Award. W.X. is supported by Alex's Lemonade Stand Foundation and the Runx1 Research Program, a Cycle for Survival's Equinox Innovation Award in Rare Cancers, MSK Leukemia

SPORE (Career Enhancement Program, NIH/NCI P50 CA254838-01) and a National Cancer Institute grant (K08CA267058-01). S.F.C. is supported by a Career Development Award from the NCI (K08CA241371-01A1). J.L.G is supported by a K08 through the National Institute of Health (CA230172). A.D.V. is supported by the National Cancer Institute (K08CA215317), an EvansMDS Discovery grant from the Edward P. Evans Foundation, a Clinical Investigator grant from the Damon Runyon Cancer Research Foundation (120-22), a Clinician Scientist Development grant from the Doris Duke Charitable Foundation, and grants from the Columbia University Vagelos College of Physicians & Surgeons (Gerstner Scholar and Early Career Physician Scientist). S.C.M. receives funding from the Swiss National Science Foundation (PZ00P3_161145, PCEFP3_181357), the Cancer League Basel and the “Stiftung für krebskranke Kinder Regio Basiliensis” (KLbB-4784-02-2019), and the Foundation for the Fight against Cancer. D.A.L. is supported by the Burroughs Wellcome Fund Career Award for Medical Scientists, Valle Scholar Award, Leukemia Lymphoma Scholar Award, the MacMillan Family Foundation and the MacMillan Center for the Study of the Non-Coding Cancer Genome at the New York Genome Center, and the Mark Foundation Emerging Leader Award as well as the Tri-Institutional Stem Cell Initiative, the National Heart Lung and Blood Institute (R01HL145283; R01HL157387-01A1), the National Cancer Institute (R33 CA267219), the National Human Genome Research Institute, Center of Excellence in Genomic Science (RM1HG011014) and the National Institutes of Health Common Fund Somatic Mosaicism Across Human Tissues (UG3NS132139). Studies supported by MSK core facilities were supported in part by MSKCC Support Grant/Core Grant P30 CA008748 and the Marie-Josée and Henry R. Kravis Center for Molecular Oncology. R.L.L. is also supported by a Leukemia & Lymphoma Society Specialized Center of Research grant.

REFERENCES

1. Levine RL, Pardanani A, Tefferi A, Gilliland DG. Role of JAK2 in the pathogenesis and therapy of myeloproliferative disorders. Nat Rev Cancer **2007**;7(9):673-83 doi 10.1038/nrc2210.
2. Mullally A, Lane SW, Ball B, Megerdichian C, Okabe R, Al-Shahrour F*, et al.* Physiological Jak2V617F expression causes a lethal myeloproliferative neoplasm with differential effects on hematopoietic stem and progenitor cells. Cancer Cell **2010**;17(6):584-96 doi 10.1016/j.ccr.2010.05.015.
3. Mullally A, Poveromo L, Schneider RK, Al-Shahrour F, Lane SW, Ebert BL. Distinct roles for long-term hematopoietic stem cells and erythroid precursor cells in a murine model of Jak2V617F-mediated polycythemia vera. Blood **2012**;120(1):166-72 doi 10.1182/blood-2012-01-402396.
4. Bhagwat N, Koppikar P, Keller M, Marubayashi S, Shank K, Rampal R*, et al.* Improved targeting of JAK2 leads to increased therapeutic efficacy in myeloproliferative neoplasms. Blood **2014**;123(13):2075-83 doi 10.1182/blood-2014-01-547760.
5. Yan D, Hutchison RE, Mohi G. Critical requirement for Stat5 in a mouse model of polycythemia vera. Blood **2012**;119(15):3539-49 doi 10.1182/blood-2011-03-345215.
6. Chapeau EA, Mandon E, Gill J, Romanet V, Ebel N, Powajbo V*, et al.* A conditional inducible JAK2V617F transgenic mouse model reveals myeloproliferative disease that is reversible upon switching off transgene expression. PLoS One **2019**;14(10):e0221635 doi 10.1371/journal.pone.0221635.
7. Castagnetti F, Gugliotta G, Breccia M, Stagno F, Iurlo A, Albano F*, et al.* Long-term outcome of chronic myeloid leukemia patients treated frontline with imatinib. Leukemia **2015**;29(9):1823-31 doi 10.1038/leu.2015.152.
8. Harrison CN, Vannucchi AM, Kiladjian JJ, Al-Ali HK, Gisslinger H, Knoops L*, et al.* Long-term findings from COMFORT-II, a phase 3 study of ruxolitinib vs best available therapy for myelofibrosis. Leukemia **2016**;30(8):1701-7 doi 10.1038/leu.2016.148.
9. Deininger M, Radich J, Burn TC, Huber R, Paranagama D, Verstovsek S. The effect of long-term ruxolitinib treatment on JAK2p.V617F allele burden in patients with myelofibrosis. Blood **2015**;126(13):1551-4 doi 10.1182/blood-2015-03-635235.
10. Andreoli A, Verger E, Robin M, Raffoux E, Zini JM, Rousselot P, *et al*. Clinical resistance to ruxolitinib is more frequent in patients without MPN-associated mutations and is rarely due to mutations in the JAK2 kinase drug-binding domain. Blood **2013**;122(21):1591.
11. Brkic S, Meyer SC. Challenges and Perspectives for Therapeutic Targeting of Myeloproliferative Neoplasms. Hemasphere **2021**;5(1):e516 doi 10.1097/HS9.0000000000000516.
12. Koppikar P, Bhagwat N, Kilpivaara O, Manshouri T, Adli M, Hricik T*, et al.* Heterodimeric JAK-STAT activation as a mechanism of persistence to JAK2 inhibitor therapy. Nature **2012**;489(7414):155-9 doi 10.1038/nature11303.
13. Stivala S, Codilupi T, Brkic S, Baerenwaldt A, Ghosh N, Hao-Shen H*, et al.* Targeting compensatory MEK/ERK activation increases JAK inhibitor efficacy in myeloproliferative neoplasms. J Clin Invest **2019**;129(4):1596-611 doi 10.1172/JCI98785.
14. Jayavelu AK, Schnoder TM, Perner F, Herzog C, Meiler A, Krishnamoorthy G*, et al.* Splicing factor YBX1 mediates persistence of JAK2-mutated neoplasms. Nature **2020**;588(7836):157-63 doi 10.1038/s41586-020-2968-3.
15. Anastassiadis K, Fu J, Patsch C, Hu S, Weidlich S, Duerschke K*, et al.* Dre recombinase, like Cre, is a highly efficient site-specific recombinase in E. coli, mammalian cells and mice. Dis Model Mech **2009**;2(9-10):508-15 doi 10.1242/dmm.003087.

16. Sauer B. Inducible gene targeting in mice using the Cre/lox system. Methods **1998**;14(4):381-92 doi 10.1006/meth.1998.0593.
17. Akada H, Akada S, Hutchison RE, Sakamoto K, Wagner KU, Mohi G. Critical role of Jak2 in the maintenance and function of adult hematopoietic stem cells. Stem Cells **2014**;32(7):1878-89 doi 10.1002/stem.1711.
18. Grisouard J, Hao-Shen H, Dirnhofer S, Wagner KU, Skoda RC. Selective deletion of Jak2 in adult mouse hematopoietic cells leads to lethal anemia and thrombocytopenia. Haematologica **2014**;99(4):e52-4 doi 10.3324/haematol.2013.100016.
19. Parganas E, Wang D, Stravopodis D, Topham DJ, Marine JC, Teglund S*, et al.* Jak2 is essential for signaling through a variety of cytokine receptors. Cell **1998**;93(3):385-95 doi 10.1016/s0092-8674(00)81167-8.
20. Neubauer H, Cumano A, Muller M, Wu H, Huffstadt U, Pfeffer K. Jak2 deficiency defines an essential developmental checkpoint in definitive hematopoiesis. Cell **1998**;93(3):397-409 doi 10.1016/s0092-8674(00)81168-x.
21. Madisen L, Zwingman TA, Sunkin SM, Oh SW, Zariwala HA, Gu H*, et al.* A robust and high-throughput Cre reporting and characterization system for the whole mouse brain. Nat Neurosci **2010**;13(1):133-40 doi 10.1038/nn.2467.
22. Poulos MG, Crowley MJP, Gutkin MC, Ramalingam P, Schachterle W, Thomas JL*, et al.* Vascular Platform to Define Hematopoietic Stem Cell Factors and Enhance Regenerative Hematopoiesis. Stem Cell Reports **2015**;5(5):881-94 doi 10.1016/j.stemcr.2015.08.018.
23. Socolovsky M, Nam H, Fleming MD, Haase VH, Brugnara C, Lodish HF. Ineffective erythropoiesis in Stat5a(-/-)5b(-/-) mice due to decreased survival of early erythroblasts. Blood **2001**;98(12):3261-73 doi 10.1182/blood.v98.12.3261.
24. Plummer NW, Evsyukova IY, Robertson SD, de Marchena J, Tucker CJ, Jensen P. Expanding the power of recombinase-based labeling to uncover cellular diversity. Development **2015**;142(24):4385-93 doi 10.1242/dev.129981.
25. Verstovsek S, Kantarjian H, Mesa RA, Pardanani AD, Cortes-Franco J, Thomas DA*, et al.* Safety and efficacy of INCB018424, a JAK1 and JAK2 inhibitor, in myelofibrosis. N Engl J Med **2010**;363(12):1117-27 doi 10.1056/NEJMoa1002028.
26. Fisher DAC, Miner CA, Engle EK, Hu H, Collins TB, Zhou A*, et al.* Cytokine production in myelofibrosis exhibits differential responsiveness to JAK-STAT, MAP kinase, and NFkappaB signaling. Leukemia **2019**;33(8):1978-95 doi 10.1038/s41375-019-0379-y.
27. Andrews NC, Erdjument-Bromage H, Davidson MB, Tempst P, Orkin SH. Erythroid transcription factor NF-E2 is a haematopoietic-specific basic-leucine zipper protein. Nature **1993**;362(6422):722-8 doi 10.1038/362722a0.
28. Zhao B, Mei Y, Cao L, Zhang J, Sumagin R, Yang J*, et al.* Loss of pleckstrin-2 reverts lethality and vascular occlusions in JAK2V617F-positive myeloproliferative neoplasms. J Clin Invest **2018**;128(1):125-40 doi 10.1172/JCI94518.
29. Krantz SB. Erythropoietin. Blood **1991**;77(3):419-34.
30. Dilip D, Menghrajani K, Melnick A, Elemento O, Levine RL, Glass JL. Single Cell ATAC Lineage Deconvolution Reveals Overlapping Subclones in Epigenetically Distinct AML Samples. Blood **2021**;138:2381 doi https://doi.org/10.1182/blood-2021-154517.
31. Starr R, Willson TA, Viney EM, Murray LJ, Rayner JR, Jenkins BJ*, et al.* A family of cytokine-inducible inhibitors of signalling. Nature **1997**;387(6636):917-21 doi 10.1038/43206.
32. van der Lugt NM, Domen J, Verhoeven E, Linders K, van der Gulden H, Allen J, Berns A. Proviral tagging in E mu-myc transgenic mice lacking the Pim-1 proto-oncogene leads to compensatory activation of Pim-2. EMBO J **1995**;14(11):2536-44 doi 10.1002/j.1460-2075.1995.tb07251.x.

33. Sasaki A, Yasukawa H, Suzuki A, Kamizono S, Syoda T, Kinjyo I*, et al.* Cytokine-inducible SH2 protein-3 (CIS3/SOCS3) inhibits Janus tyrosine kinase by binding through the N-terminal kinase inhibitory region as well as SH2 domain. Genes Cells **1999**;4(6):339-51 doi 10.1046/j.1365-2443.1999.00263.x.
34. Meyer SC, Keller MD, Chiu S, Koppikar P, Guryanova OA, Rapaport F*, et al.* CHZ868, a Type II JAK2 Inhibitor, Reverses Type I JAK Inhibitor Persistence and Demonstrates Efficacy in Myeloproliferative Neoplasms. Cancer Cell **2015**;28(1):15-28 doi 10.1016/j.ccell.2015.06.006.
35. Karin M. The regulation of AP-1 activity by mitogen-activated protein kinases. J Biol Chem **1995**;270(28):16483-6 doi 10.1074/jbc.270.28.16483.
36. Ortmann CA, Kent DG, Nangalia J, Silber Y, Wedge DC, Grinfeld J*, et al.* Effect of mutation order on myeloproliferative neoplasms. N Engl J Med **2015**;372(7):601-12 doi 10.1056/NEJMoa1412098.
37. Chen E, Schneider RK, Breyfogle LJ, Rosen EA, Poveromo L, Elf S*, et al.* Distinct effects of concomitant Jak2V617F expression and Tet2 loss in mice promote disease progression in myeloproliferative neoplasms. Blood **2015**;125(2):327-35 doi 10.1182/blood-2014-04-567024.
38. Kameda T, Shide K, Yamaji T, Kamiunten A, Sekine M, Taniguchi Y*, et al.* Loss of TET2 has dual roles in murine myeloproliferative neoplasms: disease sustainer and disease accelerator. Blood **2015**;125(2):304-15 doi 10.1182/blood-2014-04-555508.
39. Shepherd MS, Li J, Wilson NK, Oedekoven CA, Li J, Belmonte M*, et al.* Single-cell approaches identify the molecular network driving malignant hematopoietic stem cell self-renewal. Blood **2018**;132(8):791-803 doi 10.1182/blood-2017-12-821066.
40. Moran-Crusio K, Reavie L, Shih A, Abdel-Wahab O, Ndiaye-Lobry D, Lobry C*, et al.* Tet2 loss leads to increased hematopoietic stem cell self-renewal and myeloid transformation. Cancer Cell **2011**;20(1):11-24 doi 10.1016/j.ccr.2011.06.001.
41. Vasan N, Baselga J, Hyman DM. A view on drug resistance in cancer. Nature **2019**;575(7782):299-309 doi 10.1038/s41586-019-1730-1.
42. Meyer SC. Mechanisms of Resistance to JAK2 Inhibitors in Myeloproliferative Neoplasms. Hematol Oncol Clin North Am **2017**;31(4):627-42 doi 10.1016/j.hoc.2017.04.003.
43. Wu SC, Li LS, Kopp N, Montero J, Chapuy B, Yoda A*, et al.* Activity of the Type II JAK2 Inhibitor CHZ868 in B Cell Acute Lymphoblastic Leukemia. Cancer Cell **2015**;28(1):29-41 doi 10.1016/j.ccell.2015.06.005.
44. Reis E, Celik H, Marty C, Lei A, Jobe F, Rupar M, *et al*. Discovery of INCA033989, a Monoclonal Antibody That Selectively Antagonizes Mutant Calreticulin Oncogenic Function in Myeloproliferative Neoplasms (MPNs). Blood **2022**;140:14-5.
45. Glassman CR, Tsutsumi N, Saxton RA, Lupardus PJ, Jude KM, Garcia KC. Structure of a Janus kinase cytokine receptor complex reveals the basis for dimeric activation. Science **2022**;376(6589):163-9 doi 10.1126/science.abn8933.
46. Ruzankina Y, Pinzon-Guzman C, Asare A, Ong T, Pontano L, Cotsarelis G*, et al.* Deletion of the developmentally essential gene ATR in adult mice leads to age-related phenotypes and stem cell loss. Cell Stem Cell **2007**;1(1):113-26 doi 10.1016/j.stem.2007.03.002.
47. Corces MR, Buenrostro JD, Wu B, Greenside PG, Chan SM, Koenig JL*, et al.* Lineage-specific and single-cell chromatin accessibility charts human hematopoiesis and leukemia evolution. Nat Genet **2016**;48(10):1193-203 doi 10.1038/ng.3646.
48. Granja JM, Corces MR, Pierce SE, Bagdatli ST, Choudhry H, Chang HY, Greenleaf WJ. ArchR is a scalable software package for integrative single-cell chromatin accessibility analysis. Nat Genet **2021**;53(3):403-11 doi 10.1038/s41588-021-00790-6.

941 49. Schep AN, Wu B, Buenrostro JD, Greenleaf WJ. chromVAR: inferring transcription-
942 factor-associated accessibility from single-cell epigenomic data. Nat Methods
943 **2017**;14(10):975-8 doi 10.1038/nmeth.4401.
944
945
946
947

AUTHOR CONTRIBUTIONS

A.D., R.L.B. and R.L.L. conceived the project, designed the experiments, and analyzed the data. *In vivo* work was performed primarily by A.D. with technical assistance from Y.P., K.O. A.K., W.J.K., Z.Z., A.N, M.B, M.F, T.C., S.C., A.H., L.C., B.W., W.A., S.M., S.E., T.M.. Additional project design provided by A.V. and S.C.M.. Hematopathology was formally interpreted by W.X.. Bone marrow endothelial experiments were performed by A.D., M.W., and I.F.M.. R.L.B., J.Y, J.L.G., and R.K. performed the computational analysis. Single-cell human ATAC data was performed and analyzed primarily by F.I., R.M.M, with support from D.L.. A.D., R.L.B., and R.L.L. contributed to the initial manuscript drafts. All authors reviewed and commented on the final manuscript. Funding acquisition: R.L.L., D.L., A.D., and R.L.B..

MATERIALS AND CORRESPONDENCE

Correspondence and requests for materials should be addressed to R.L.L.

Figure 1: *Jak2*^{V617F} deletion abolishes JAK/STAT signaling and abrogates the MPN phenotype. A) Schematic representation of the dual-recombinase *Jak2*^{V617F} conditional knock-in/knock-out allele (*Jak2*^{RL}), the *Jak2*^{RL} knock-in allele following Dre recombination, and the null recombined allele following Cre-mediated deletion. Semi-circles indicate *Rox* sequences; triangles indicate *lox*P sequences. **B)** Representative western blot depicting phospho-STAT5 abundance of Dre-mediated *Jak2*^{V617F} knock-in (+Dre) vs. *Jak2*^{V617F}-deleted (+Dre +Cre) states from isolated splenocytes 7 days following TAM administration in comparison to unrecombined (Unrec.) *Jak2*^{RL} cells ($n = 2$ biological replicates each; representative of $n = 2$ independent experiments). **C)** Peripheral blood count trends (weeks 0-24) of MPN vs. TAM (*Jak2*^{V617F}-deleted) treated mice: white blood cells (WBC; left panel), hematocrit (Hct; right panel) ($n \geq 10$ per arm; mean ± s.e.m). Gray bar represents duration of TAM pulse/chow administration. Representative of $n = 2$ independent transplants. $^{**}p \leq 0.01$, $^{****}p \leq 0.0001$. **D)** Kaplan–Meier survival analysis of MPN vs. TAM (*Jak2*^{V617F}-deleted) treated mice ($n \geq 12$ per arm; Log-rank test). Gray bar represents duration of TAM pulse/chow administration. $^{****}p \leq 0.0001$. **E)** Spleen weights of MPN vs. TAM (*Jak2*^{V617F}-deleted) treated mice at timed sacrifice (24 weeks) in comparison to wild-type (WT) control mice (mean ± s.e.m.). Representative of $n = 2$ independent transplants. $^{****}p \leq 0.0001$. **F)** Heatmap scaled using Z-scores of serum cytokine/chemokine concentrations of MPN vs. TAM (*Jak2*^{V617F}-deleted) treated mice harvested at time of sacrifice 18-24 weeks post-transplant in comparison to WT control mice ($n = 4$-7 biological replicates per arm pooled from $n = 3$ transplants). Asterisks denote cytokines with $FDR \leq 0.05$. Kruskal-Wallis test with FDR correction. **G)** Representative hematoxylin and eosin (H&E) and reticulin stains of bone marrow of MPN (Control) vs. TAM (*Jak2*^{V617F}-deleted) treated mice from timed sacrifice 24 weeks. Representative micrographs of $n = 6$ individual mouse replicates per arm. All images represented at 400X magnification. Scale bar: 20μm.

Figure 2: *Jak2*^{V617F} reversal impairs the fitness of MPN cells, including MPN stem cells. A) Peripheral blood (PB) mutant Cd45.2 percent chimerism trend (weeks 0-24) of early (3 weeks post-transplant) TAM (*Jak2*^{V617F}-deleted) treated (gold bar) and late (12 weeks post-transplant) TAM treated (maroon bar) mice (*n* = 8 each) in comparison to MPN (dark gray bar; *n* = 6) mice (mean ± s.e.m.). Gray bars represent duration of TAM pulse/chow administration. Representative of *n* = 2 independent transplants. ***p* ≤ 0.01, ****p* ≤ 0.001. **B)** Bone marrow mutant cell fraction within LSK (Lineage$^-$Sca1$^+$cKit$^+$), granulocytic-monocytic progenitor (GMP; Lineage$^-$cKit$^+$Sca1$^-$Cd34$^+$Fcg$^+$), and megakaryocytic-erythroid progenitor (MEP; Lineage$^-$cKit$^+$Sca1$^-$Cd34$^-$Fcg$^-$) compartments of early (3 weeks post-transplant) TAM (*Jak2*^{V617F}-deleted) treated and late (12 weeks post-transplant) TAM treated mice in comparison to MPN mice at timed sacrifice 24 weeks (*n* = 6-8 individual biological replicates per arm; mean ± s.e.m.). Representative of *n* = 2 independent transplants. ***p* ≤ 0.01, ****p* ≤ 0.001, *****p* ≤ 0.0001. **C)** Gene-set enrichment analysis (GSEA) of significant Hallmark gene sets of MPN vs. TAM (*Jak2*^{V617F}-deleted) treated LSKs isolated 7 days following initiation of TAM (*n* = 3-4 biological replicates per arm). **D)** Volcano plot demonstrating differential gene expression of MPN vs. TAM (*Jak2*^{V617F}-deleted) treated LSKs 7 days following initiation of TAM (*n* = 3-4 biological replicates per arm). **E)** GMP and MEP stem cell frequencies of MPN vs. TAM (*Jak2*^{V617F}-deleted) treated mice 7 days following initiation of TAM (*n* = 8 biological replicates per arm across 2 independent transplants; mean ± s.e.m.). **F)** Row normalized heatmap of RNA-Seq data of key erythroid differentiation factor genes from harvested MEPs at baseline (MPN), day 3 (D3) and day 7 (D7) following initiation of TAM (*Jak2*^{V617F} deletion). **G)** HOMER motif analysis from ATAC-Seq data demonstrating decreased accessibility of Gata motif signatures with concomitant increased accessibility of Cebp motif signatures of TAM treated (*Jak2*^{V617F}-deleted) cKit$^+$ bone marrow cells isolated 7 days following initiation of treatment in comparison to MPN cells (*n* = 3 biological replicates per arm).

Figure 3: Differential efficacy of *Jak2*^{V617F} deletion compared to JAK inhibitor therapy. A) Scatter plot depicting -log10(adjusted p vale)*sign(log2FoldChange) of ruxolitinib (RUX) treated vs. TAM (*Jak2*^{V617F}-deleted) treated LSKs (Lineage$^-$Sca1$^+$cKit$^+$) in comparison to MPN control LSKs isolated after 7 days of treatment (n = 2-3 biological replicates per arm); differentially expressed genes as indicated by color (see Supplemental Tables 1 and 3). **B)** Gene set enrichment analysis (GSEA) depicting a positive enrichment in heme metabolism in RUX treated (n = 3) vs. negative enrichment in TAM (*Jak2*^{V617F}-deleted) treated (n = 3) LSKs isolated after 7 days of treatment. **C)** Box plot of the top leading edge genes in the Hallmark heme metabolism gene set of RUX treated (blue) or TAM (*Jak2*^{V617F}-deleted) treated (red) megakaryocytic-erythroid progenitor (MEP; Lineage$^-$cKit$^+$Sca1$^-$Cd34$^-$Fcg$^-$) cells as compared to untreated MPN cohorts. **D)** Box plots of single-cell ATAC-Seq motif accessibility for either NFKB1 or REL transcription factors for untreated human *JAK2* WT (n = 188 cells from 4 patients; gray), untreated *JAK2*^{V617F}-mutant (n = 105 cells from 4 patients; gray), and RUX-treated *JAK2*^{V617F}-mutant (n = 87 cells from 3 patients; blue) HSPCs (from Myers, R.M. and Izzo, F. *et al*., *Nature, in press,* 2024). *P* values indicated are from linear mixture model explicitly modeling patient identity as random effect to account for patient-specific effects, followed by likelihood ratio test. ****$p \leq 0.0001$. **E)** Peripheral blood counts of VEH, RUX, the type II JAK2 inhibitor CHZ868 (CHZ), or TAM (*Jak2*^{V617F}-deleted) treated mice at the conclusion of a 6-week *in vivo* trial: white blood cells (WBC; left panel), hematocrit (Hct; right panel) ($n \geq 4$ each; mean ± s.e.m). **$p \leq 0.01$, ***$p \leq 0.001$, ****$p \leq 0.0001$. **F)** Peripheral blood (PB) mutant Cd45.2 percent chimerism trend (0-6 weeks) of VEH, RUX, CHZ868 (CHZ), or TAM (*Jak2*^{V617F}-deleted) treated mice ($n \geq 4$ each; mean ± s.e.m.). *$p \leq 0.05$. **G)** Bone marrow mutant cell fraction of LSK (Lineage$^-$Sca1$^+$cKit$^+$), granulocytic-monocytic progenitor (GMP; Lineage$^-$cKit$^+$Sca1$^-$Cd34$^+$Fcg$^+$), and megakaryocytic-erythroid progenitor (MEP; Lineage$^-$cKit$^+$Sca1$^-$Cd34$^-$Fcg$^-$) compartments of VEH, RUX, CHZ868 (CHZ), or TAM (*Jak2*^{V617F}-deleted) treated mice at the conclusion of the 6-week *in vivo* trial ($n \geq 4$ each; mean ± s.e.m). *$p \leq 0.05$, ****$p \leq 0.0001$. **H)** GSEA depicting a negative enrichment in down-regulation of KRAS signaling targets in RUX treated (n = 3) vs. positive enrichment in TAM (*Jak2*^{V617F}-deleted) treated (n = 3) MEPs isolated following 7 days of respective treatment. **I)** Immunohistochemistry of phospho-ERK on sectioned bone marrow of VEH, RUX, or TAM (*Jak2*^{V617F}-deleted) treated mice following 7 days of treatment (n = 3 individual biological replicates per arm). All images represented at 400X magnification. Scale bar: 20μm. **J)** Quantitative polymerase-chain reaction demonstrating relative *Ybx1* expression levels from isolated cKit$^+$ bone marrow of VEH vs. RUX vs. TAM (*Jak2*^{V617F}-deleted) treated mice following 7 days of treatment (n = 2-4 individual biological

replicates per arm; mean ± s.e.m). *$p \leq 0.05$, **$p \leq 0.01$. **E-G)** Representative of $n = 3$ independent experiments.

Figure 4: Jak2^{V617F} dependency with cooperative Tet2 loss. A) Schematic of the experimental set up for the double-mutant *Jak2^{RL}/Tet2$^{f/f}$* competitive transplants. TAM: tamoxifen; KI: knock-in; KO: knock-out; Lin-neg BM: lineage-negative bone marrow; cGy: centigray. Downward arrows represent initial pulse TAM administration to genetically inactivate *Tet2*. **B)** White blood cell (WBC) counts of primary *Jak2^{RL}* vs. *Tet2$^{-/-}$* vs. *Jak2^{RL}/Tet2$^{-/-}$* transplanted mice at 16 weeks post-transplant (n = 5-6 each; mean ± s.e.m.). Representative of an n = 2 independent transplants. *$p \leq 0.05$, ***$p \leq 0.001$. **C)** Spleen weights of primary *Jak2^{RL}* vs. *Tet2$^{-/-}$* vs. *Jak2^{RL}/Tet2$^{-/-}$* transplanted mice at time of sacrifice (n = 5-6 each; mean ± s.e.m.). Representative of an n = 2 independent transplants. *$p \leq 0.05$, **$p \leq 0.01$. **D)** Peripheral blood Cd45.2 mutant percent chimerism of *Jak2^{RL}* vs. *Tet2$^{-/-}$* vs. *Jak2^{RL}/Tet2$^{-/-}$* secondary competitive transplant mice at 9 weeks post-transplant ($n \geq 10$ per arm; mean ± s.e.m.). Representative of an n = 2 independent transplants. *$p \leq 0.05$. **E)** Peripheral blood count trends (weeks 0-21) of MPN vs. TAM (*Jak2^{V617F}*-deleted) treated *Jak2^{RL}* vs. *Jak2^{RL}/Tet2$^{-/-}$* competitive transplant mice: white blood cells (WBC; left panel), hematocrit (Hct; right panel) (n = 3-4 per arm; mean ± s.e.m). Gray bars represent duration of TAM pulse/chow administration. Representative of n = 2 independent transplants. **$p \leq 0.01$, ***$p \leq 0.001$, ****$p \leq 0.0001$. **F)** Fold-change from baseline (pre-treatment) to post- of Cd45.2 mutant peripheral blood chimerism of *Jak2^{RL}* vs. *Tet2$^{-/-}$* vs. *Jak2^{RL}/Tet2$^{-/-}$* transplanted mice treated for 6 weeks with either VEH, RUX (60mg/kg BID), or TAM (*Jak2^{VF}* deletion) (n = 4-5 per arm; mean ± s.e.m.). *$p \leq 0.05$. **G)** Reticulin stains of bone marrow from MPN vs. TAM (*Jak2^{V617F}*-deleted) treated *Jak2^{RL}* vs. *Jak2^{RL}/Tet2$^{-/-}$* mice at timed sacrifice 21 weeks. Representative micrographs of n = 3 individual mouse replicates per arm. All images represented at 400X magnification. Scale bar: 20μm. **H)** Bone marrow mutant Cd45.2 percent chimerism within the LSK (Lineage^{-}Sca1^{+}cKit^{+}) compartment of MPN vs. TAM (*Jak2^{V617F}*-deleted) treated *Jak2^{RL}* vs. *Jak2^{RL}/Tet2$^{-/-}$* mice at timed sacrifice 21 weeks ($n \geq 7$ biological replicates per arm across 2 independent transplants; mean ± s.e.m). *$p \leq 0.05$, ***$p \leq 0.001$. **I)** Serial replating assay of plated MPN vs. TAM (*Jak2^{V617F}*-deleted) treated *Jak2^{RL}* vs. *Jak2^{RL}/Tet2$^{-/-}$* bone marrow cells harvested at timed sacrifice 21 weeks and scored at day 8 after each plating (each sample plated in triplicate, representative of n = 2 independent experiments, mean ± s.d.).

Figure 1

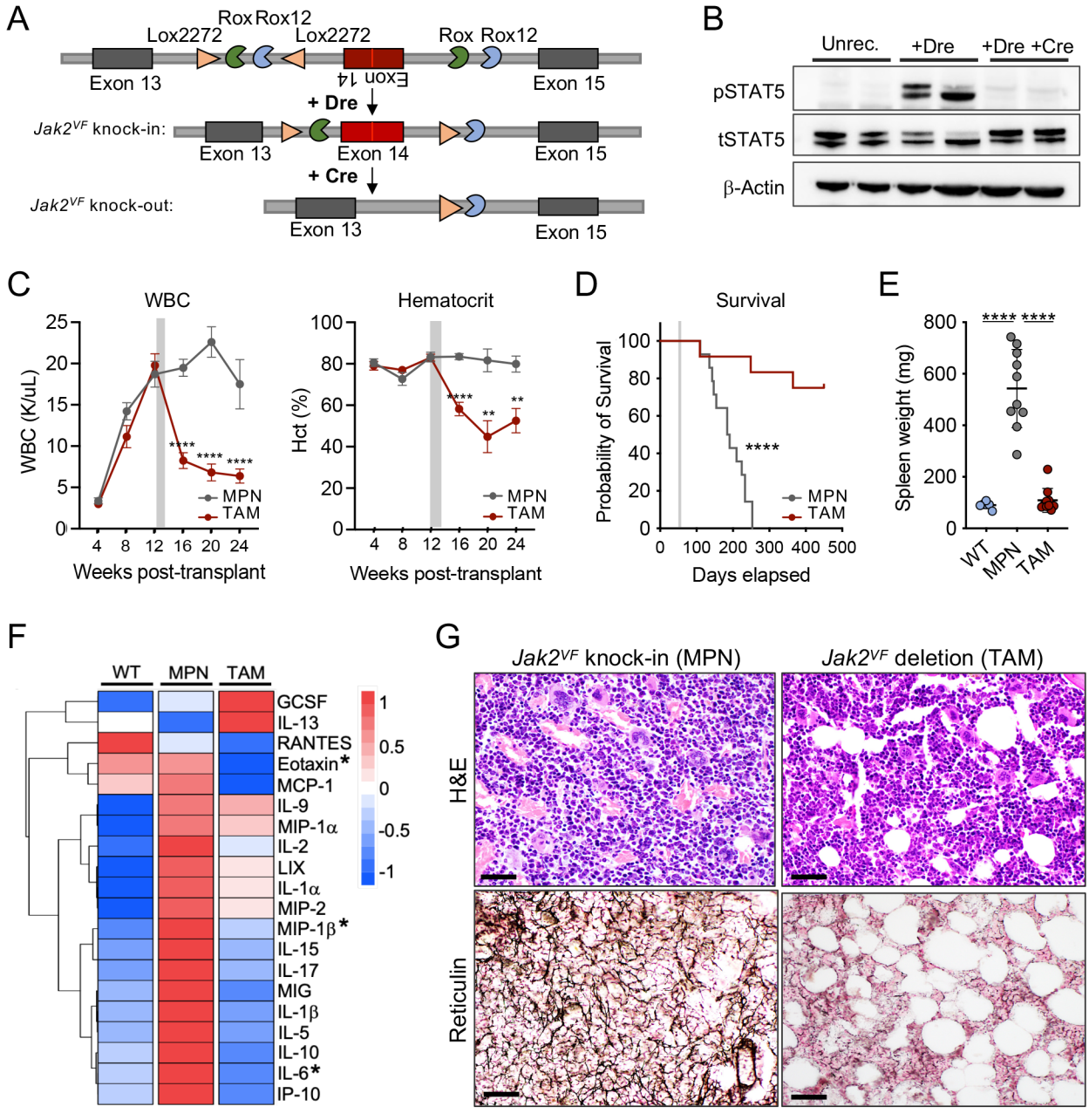

Figure 2

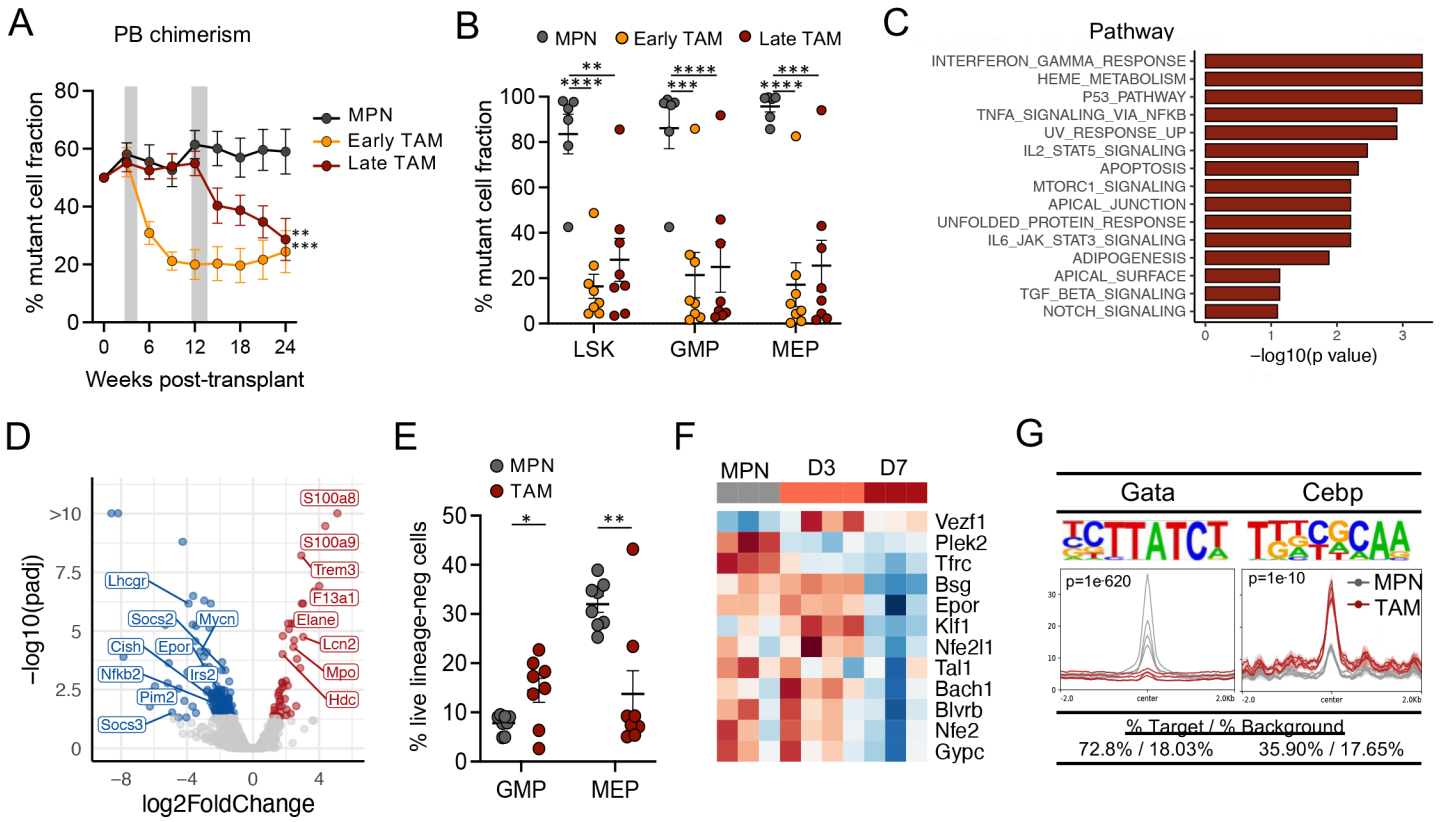

Figure 3

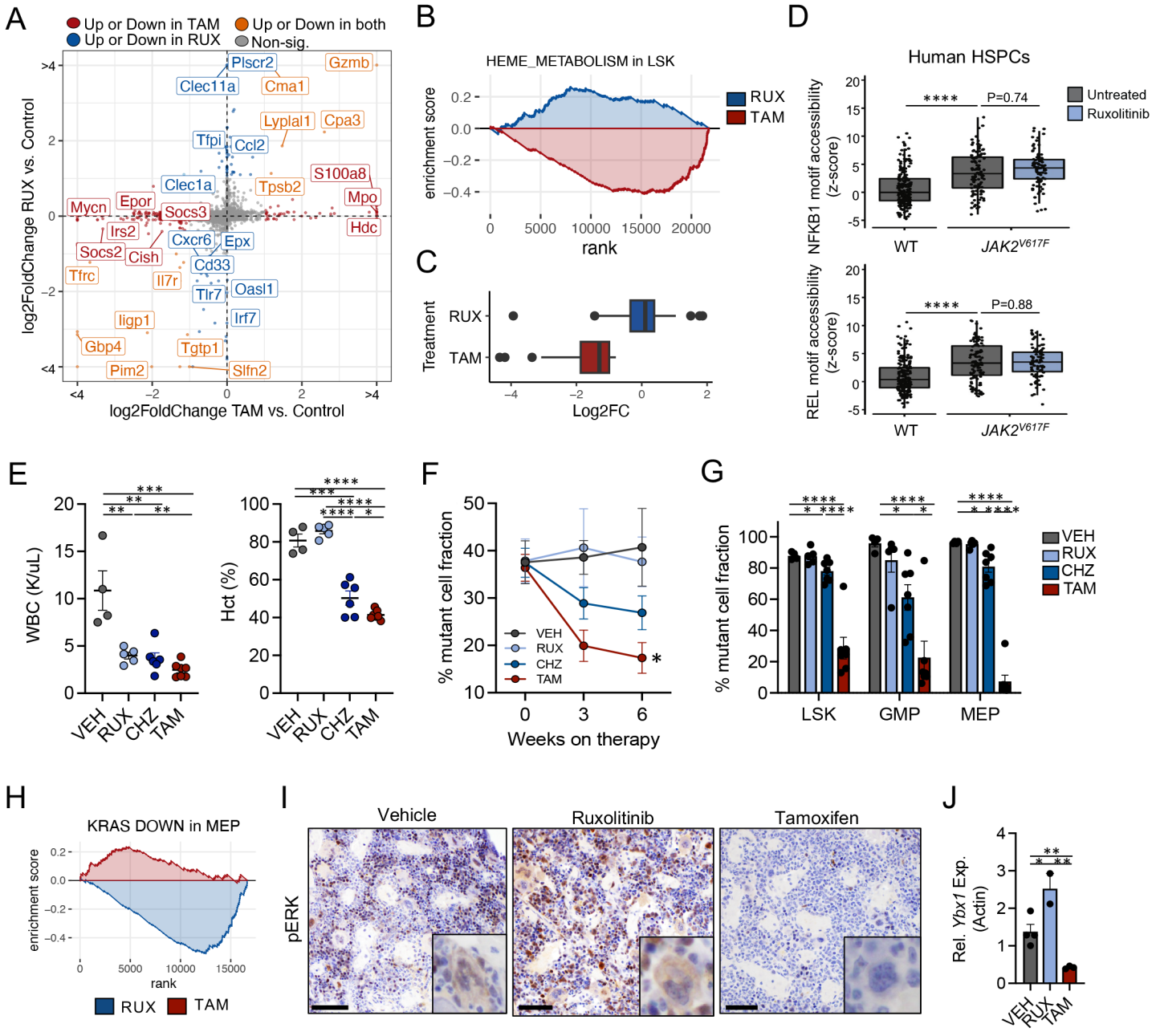

Figure 4